



A review: the development of field synergy and its application to cooling exchangers in the hot-wet mining field

Min Qu^{1,2,3} · Yongliang Zhang^{2,3} · Xilong Zhang^{2,3} · Hui Song^{2,3} · Cuicui Fu^{2,3} · Qi Yao^{2,3} · Shili Yin^{2,3}

Received: 1 October 2022 / Accepted: 18 April 2023 / Published online: 11 May 2023
© Akadémiai Kiadó, Budapest, Hungary 2023

Abstract

Convective heat and mass transfer are common phenomena in the field of engineering. In recent years, the research on convective heat and mass transfer is getting deeper and deeper. People are constantly seeking new methods to improve the efficiency of heat and mass transfer, but the research on the mechanism of heat and mass transfer is not yet systematic and mature. The theory of the field synergy has made up for this research gap, but the research progress and application of its heat and mass transfer theory lack systematic summary and evaluation. This paper summarizes the theory of enhanced heat and mass transfer based on field synergy theory, analyzes the field synergy equation of heat transfer, mass transfer, and heat-mass cooperation under laminar and turbulent conditions, and gives the evaluation standard of field synergy equation. Field synergy theory shows that improving the synergy between the velocity field and temperature gradient field, that is, reducing the angle between them, can effectively improve the heat transfer efficiency, and improving the synergy between the velocity field and concentration gradient field can effectively improve the mass transfer efficiency. Subsequently, the research progress of field synergy theory in different engineering fields is summarized. It is shown that field synergy theory can be used to analyze the cooperation between fields in heat exchangers, micro-components, nanofluids, reactors and other fields to guide the optimal design of equipment, which proves the universality of field cooperation theory. Finally, in view of the universality of the damp-heat exchange in the cooling exchangers and the research object of field synergy theory, a new idea of using the field synergy theory to guide the research on the structural design of cooling exchangers is put forward, which provides new ideas and methods for effectively improving the underground humid and thermal environment.

Keywords Heat-mass synergy · The field synergy theory · Field synergy applications · Damp and heat in the mine · Heat transfer

List of symbols

U Fluid velocity, $\text{m}\cdot\text{s}^{-1}$
 ∇T Temperature gradient, $\text{K}\cdot\text{m}^{-1}$
 a Thermal diffusivity, $\text{m}^2\cdot\text{s}^{-1}$
 Nu Nusselt number

Re Reynolds number
 Pr Prandtl number
 $\delta_{t/l}$ Thickness of thermal boundary layer, m
 ∇T Dimensionless temperature gradient
 β The angle between the velocity field and the temperature gradient field, $^\circ$
 μ Dynamic viscosity, $\text{Pa}\cdot\text{s}$
 ρ Density, $\text{kg}\cdot\text{m}^{-3}$
 C_Φ Synergy coefficient, $\text{N}\cdot(\text{m}^2\cdot\text{K})^{-1}$
 c_p Specific heat capacity at constant pressure, $\text{J}\cdot\text{kg}^{-1}\cdot\text{K}^{-1}$
 \vec{n} The outer normal of the computational domain
 N Control volume
 u, v, w The velocity components of the fluid in the x, y, and z directions, $\text{m}\cdot\text{s}^{-1}$
 $v_{i,j,k}$ Volume element, m^3
 β_m The average value of the angle between the velocity field and the temperature gradient field, $^\circ$

✉ Yongliang Zhang
zhyoliang@163.com

¹ School of Environmental and Municipal Engineering, Qingdao University of Technology, Qingdao 266520, Shandong, China

² Key Lab of Industrial Fluid Energy Conservation and Pollution Control, Ministry of Education, Qingdao University of Technology, Qingdao 266520, Shandong, China

³ School of Mechanical and Automotive Engineering, Qingdao University of Technology, Qingdao 266520, Shandong, China

Ω	Domain	h	Convective heat transfer coefficient between roadway wall and wind flow, $\text{W}\cdot(\text{m}^2\cdot\text{K})^{-1}$
k	Thermal conductivity, $\text{W}\cdot(\text{m}\cdot\text{K})^{-1}$	F_0	Fourier quasi-number, dimensionless time
q_w	Heat flux of the wall, $\text{W}\cdot\text{m}^2$	B_i	Dimensionless heat dissipation coefficient
∇C	Concentration gradient, $\text{mol}\cdot\text{m}^4$	Sh	Sherwood number
D	Concentration diffusivity, $\text{m}^2\cdot\text{s}$	$\delta_{m/l}$	The thickness of the Concentration boundary layer, m
Sc	Schmidt number	α	The angle between the velocity field and the concentration gradient field, $^\circ$
$\overline{\nabla C}$	Dimensionless concentration gradient	Y	Substance mass fraction
A_0	Lagrangian multiplication factor	ξ	Fluid power factor, $\text{kg}\cdot(\text{m}\cdot\text{s})^{-1}$
∇P	Pressure difference between inlet and outlet sections, Pa	Li	Dimensionless number, $Li = v/\xi$
Eu	Euler number	$\delta_{H,x}$	Enthalpy boundary width, m
θ	The angle between the velocity field and the pressure gradient field, $^\circ$	α_h	The angle between the velocity vector and the enthalpy gradient, $^\circ$
h_{eff1}	Heat transfer coefficient of wall-1, $\text{W}\cdot(\text{m}^2\cdot\text{K})^{-1}$	N_y	Mass transfer rate in the y-direction
∇H_v	Enthalpy gradient per unit volume	λ_{FSP}	Field synergy across the flow domain
γ	The angle between the temperature gradient and the moisture gradient, $^\circ$	χ	Heat transfer coefficient of the Cooling tower, $\text{W}\cdot(\text{m}^2\cdot\text{K})^{-1}$
Fc	Field synergy number	m_a	Mass flow of dry air, $\text{kg}\cdot\text{s}$
T	Temperature, K	i_a	Enthalpy of air, $\text{J}\cdot\text{kg}$
ζ	Mass transfer coefficient of the cooling tower, $\text{s}\cdot\text{m}^{-1}$		
h_{eff2}	Heat transfer coefficient of wall-2, $\text{W}\cdot(\text{m}^2\cdot\text{K})^{-1}$		
$\overline{Q}_{\text{wall-1}}$	Average heat transfer of wall-1, J		
R_h	Correlation Coefficient for Regression Analysis		
$\overline{Q}_{\text{wall-2}}$	Average heat transfer of wall-2, J		
$\overline{T}_{\text{wall-1}}$	Average temperature of wall-1, K		
$\overline{T}_{\text{wall-2}}$	Average temperature of wall-2, K		
T_{ref1}	Reference temperature of the evaporation section, K		
T_{ref2}	Reference temperature of condensation section, K		
$\overline{c_p}$	Average isobaric heat capacity, $\text{J}\cdot\text{kg}^{-1}\cdot\text{K}^{-1}$		
$\overline{\mu}$	Average dynamic viscosity, $\text{Pa}\cdot\text{s}$		
\overline{k}	Average thermal conductivity, $\text{W}\cdot(\text{m}\cdot\text{K})^{-1}$		
q_w	The total heat flux density of the surrounding rock to dissipate heat to the wind flow, $\text{J}\cdot(\text{s}\cdot\text{m}^2)^{-1}$		
q_s	Density of sensible heat flow into the wind flow from the roadway wall, $\text{J}\cdot(\text{s}\cdot\text{m}^2)^{-1}$		
q_l	Density of latent heat flow into the wind flow from the roadway wall, $\text{J}\cdot(\text{s}\cdot\text{m}^2)^{-1}$		
q_f	Sensible heat that increases the temperature of the air flow, $\text{J}\cdot(\text{s}\cdot\text{m}^2)^{-1}$		
q_t	Latent heat required for water evaporation in wind, $\text{J}\cdot(\text{s}\cdot\text{m}^2)^{-1}$		
s	Heat or mass transfer area, m^2		
e	Thermal conductivity of surrounding rock, $\text{W}\cdot(\text{m}^2\cdot\text{K})^{-1}$		
R_0	Equivalent Radius of the tunnel, m		

Introduction

Convective heat transfer is widely used in the engineering field. The research on heat transfer performance [1–5] has been relatively mature, mainly focusing on theoretical research and experimental measurement, which improve its heat transfer performance by enhancing the heat transfer coefficient [6]. To reveal the essence of heat transfer enhancement theoretically, Guo [7–9] proposed the concept of field synergy, pointing out that increasing the synergy between velocity field and temperature gradient field can effectively enhance heat transfer. Once the field synergy theory was put forward, it set off a new wave of research in academia. Based on the research based on parabolic flow, many scholars have extended it to elliptical flow, parabolic flow [10–13], turbulent flow [14], and so on. In addition, the research field is not only limited to heat transfer, but also the fields of mass transfer [15] and heat-mass synergy [16], and has achieved fruitful research results.

The research of basic theory is often for better application practice. At present, the field synergy theory has been widely used in engineering practice. In the initial stage, it was mainly reflected in the research on heat exchangers [17, 18]. By optimizing the heat exchanger channel structure [11, 19–21] and fins [22–26], the heat transfer performance was improved, and combining heat transfer with a desiccant [27] can achieve a good thermal-mass coupling in the area of field synergy practice, the optimized design in the area of heat exchangers also encourages the field synergy theory to

enhance heat transfer research in other areas, embodied in porous media [28], combustion reactors [29–31], nanofluids [32], screw plasticizing systems [33], closed oscillating heating pipe (COHP) [34] and other fields. The good demonstration in the area of heat exchange also promotes its research in the direction of mass transfer and heat-mass coupling, such as photocatalytic oxidation reactor (POC) [35], sea-water desalination [36], closed wet cooling tower (CWCT) [37], polysilicon chemical vapor deposition reactor [38]. More and more applications have shown that field synergy theory can enhance heat and mass transfer by optimizing structural design.

With the increase of the mining depth of the mine, the underground high temperature and high humidity environment need to be solved urgently because of its serious harm to the workers [39–42]. The setting of an underground ventilation system is the main means to reduce the high temperature and humidity environment. However, with the deepening of excavation, the underground high-temperature environment is aggravated, making the inlet temperature of the fan in the ventilation system generally higher, which seriously affects the temperature drop effect of deep well high-temperature environment. Therefore, the installation of a cooling exchanger at the front of the fan and using the cooling water to exchange the heat with the hot-wet air in the tunnel can effectively reduce the inlet temperature of the fan in the ventilation system, thereby improving the efficiency of the ventilation system and effectively improving the humid and hot environment of the deep well. Because the heat transfer mechanism of cooling heat exchangers in the deep well ventilation system is common to the research object of field synergy theory, applying it to the design and research of cooling exchangers will play an important positive role in improving the heat transfer performance.

Based on the above, this paper firstly summarizes the development research status of the field synergy theory since the field synergy theory was put forward. In the second chapter, the synergistic equations of heat and mass transfer fields under different conditions are analyzed and summarized, and the evaluation indexes of field synergistic effect are determined. In the third chapter, the research progress of field synergy theory in heat exchangers, micro-components, nanofluids, reactors and other fields is summarized, and the positive results of field synergy theory in engineering practice are explained, indicating that its theory has high universality. Finally, based on the good demonstration effect of field synergy theory in other fields, a new idea of applying it to the research and design of cooling exchangers in wet-hot mines is put forward, which provides a new idea and research direction for improving the damp hot environment of deep mine and improving the ventilation efficiency. The structure of this article is shown in Fig. 1.

Field synergy theory

The field synergy theory was first proposed by Guo [7–9] to solve the problem of convective heat transfer and reveal the essence of enhanced heat transfer. The initial research on field synergy is based on the convective heat transfer of parabolic flow. According to the heat energy conservation equation (Eq. 1), the field synergy equation (Eq. 2) and the formula for solving the synergy angle (Eq. 3) are proposed to enhance heat transfer, which reveals that the essence of strengthening heat transfer is to improve the synergy between the fluid velocity field and the temperature gradient field. Under the same boundary conditions as the velocity field and the temperature gradient field, improving the synergy between the velocity field and the temperature gradient field, that is, decreasing the synergy angle between the two can improve the synergy effect and enhance the heat transfer.

After the field synergy theory was put forward, it attracted extensive attention and research from all walks of life. The applicable conditions and scope of the theory of field synergy were explored, and different expressions emerged [43]. Meng [44] deduced the field synergy equation under the given viscous dissipation condition (Eq. 4) which used the variational principle, considered the viscous dissipation effect of the fluid, and took the minimum heat transfer potential capacity dissipation as the optimization objective; Liu [45, 46] extended the fluid from laminar flow to more general turbulent flow and established a three-field synergistic form of velocity field, temperature gradient field, and pressure gradient field; Tao, He [10–13] extended the applicability of the field synergy theory to elliptical flow and parabolic flow, and derived the field synergy equation (Eq. 5) and its synergy angle (Eq. 6) which shows that improving the synergy of the velocity field and the temperature gradient field can significantly improve the heat transfer ability. And according to the actual situation, the mathematical expression of the field synergy equation (Eq. 7) and the calculation formula of the average synergy angle (Eq. 8) of the laminar incompressible steady-state fluid are given; E [34] gave the field synergy effect, that is, the field synergy angle expression (Eq. 9) of the entire flow domain under the two-dimensional elliptical fluid heat transfer model (Fig. 2) based on the research of Tao, He; Guo [14] proposed that the field synergy theory is also applicable to turbulent flow, and deduced the field synergy equation for turbulent pipelines (Eq. 10). Most of the research and evaluation methods on field synergy usually use the value of the average field synergy angle as an index to evaluate the synergy effect. However, based on the instantaneous change of the velocity field and the temperature gradient field in the fluid flow process, the field structure is relatively complex, and the evaluation standard of the average field synergy angle has limitations,

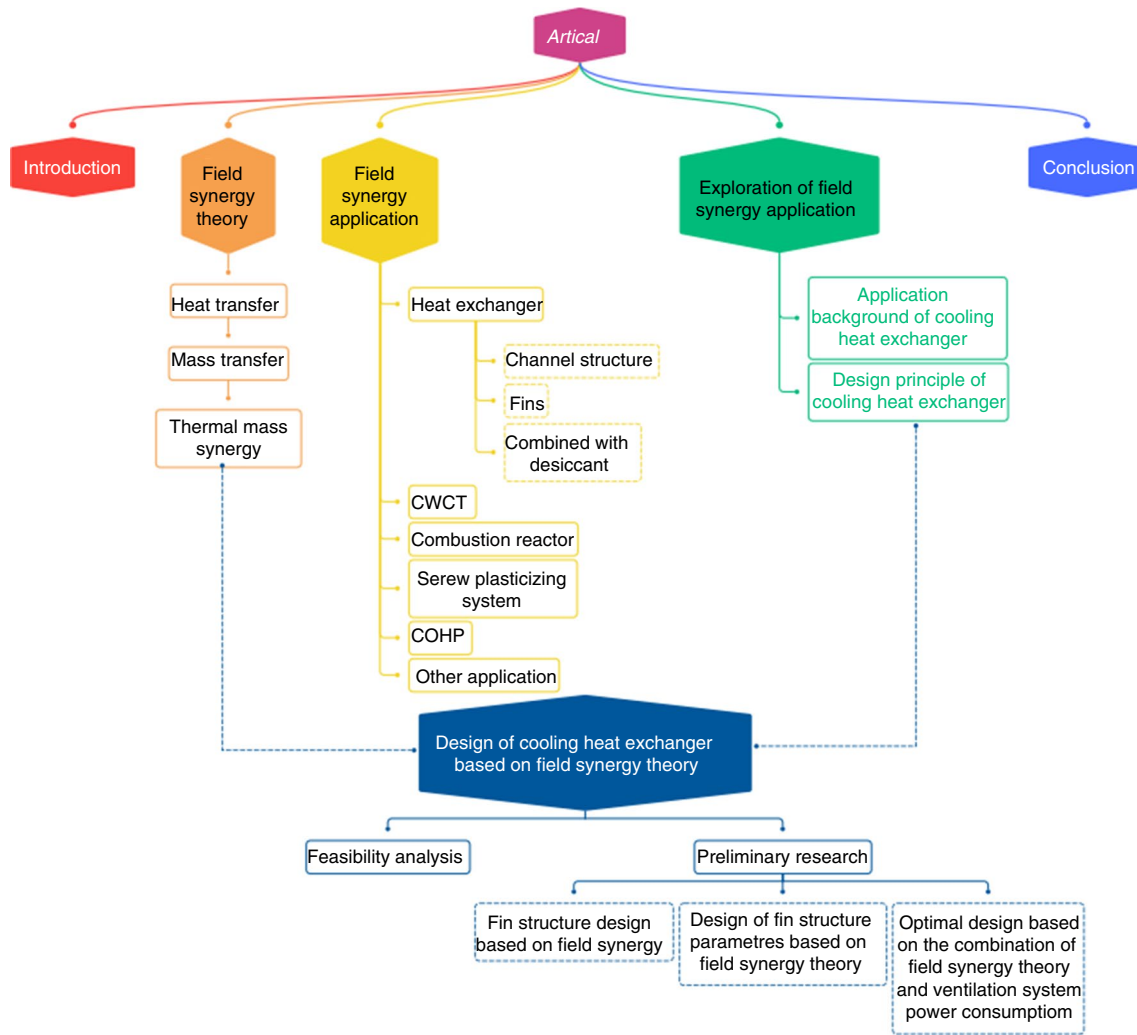
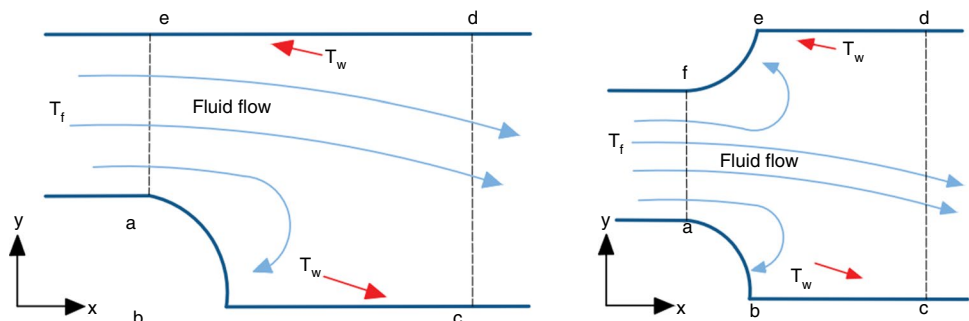


Fig. 1 Article structure

Fig. 2 Two-dimensional elliptical fluid flow heat transfer model (T_w is the wall temperature; T_f is the fluid temperature; a, b, c, d, e, f is endpoints of different sections)



which cannot reflect the enhance the heat transfer effect when the velocity and temperature gradient are small. To this end, the dimensionless number F_c is introduced as the field synergy number (Eq. 11), and its value ranges from 0 to 1, which is used to express the degree of synergy between the velocity field and the temperature gradient field [14].

The field synergy theory is not only applicable to the field of enhanced heat transfer based on convective heat transfer but also can reveal the principle of enhanced mass transfer [15]. According to the different properties of the fluid medium, different mass transfer field synergy equations are established. The most common field synergy theory of

convective mass transfer is the study of fluid component concentrations. Liu [47] first derived the mass transfer synergy equation of component concentration (Eq. 13) and its synergy angle (Eq. 14) based on thermal energy conservation and then established synergy equations based on heat conservation, mechanical energy conservation, component mass conservation, and fluid mass conservation, revealing the multi-field system relationship among velocity field, pressure field, temperature gradient field, and component concentration field, which analyzed the physical properties

of the enhanced tube convective mass transfer. The established mechanical energy conservation (Eq. 15), field synergy equation (Eq. 16), and synergy angle formula (Eq. 17) are shown in Table 1. Chen [35] deduced the field synergy equation (Eq. 18) with specific conditions based on the principle of mass transfer potential capacity dissipation extremum when using ultraviolet radiation to study photocatalytic reactors. Under given boundary conditions, the optimal velocity field with a high mass transfer rate can be obtained by solving the equation.

Table 1 Equations of the field synergy theory

Equation	Parameter	Number
$\vec{U} \cdot \nabla T = a \nabla^2 T$	$\vec{U}; \nabla T; a$	Equation 1
$Nu = Re Pr \int_0^{\delta_{m/l}} (\vec{U} \cdot \nabla \vec{T}) dY$	$Nu; Re; Pr; \delta_{m/l}; \nabla \vec{T}$	Equation 2
$\beta = \arccos \frac{\vec{U} \cdot \nabla T}{ \vec{U} \nabla T }$	$\beta; \vec{U}; \nabla T$	Equation 3
$\mu \nabla^2 \vec{U} - \rho \vec{U} \cdot \nabla \vec{U} - \nabla P + (C_\Phi A \nabla T + \rho \vec{U} \cdot \nabla \vec{U}) = 0$	$\mu; \vec{U}; \rho; C_\Phi$	Equation 4
$\int_\Omega \rho c_p (\vec{U} \cdot \text{grad} T) dA = \int_{bcd} \lambda \vec{n} \cdot \nabla T ds + \int_{efa} \lambda \vec{n} \cdot \nabla T ds$	$\rho; c_p; \vec{U}; \nabla T; \vec{n}$	Equation 5
$\beta = \cos^{-1} \frac{u \frac{\partial T}{\partial x} + v \frac{\partial T}{\partial y} + w \frac{\partial T}{\partial z}}{ \vec{U} \nabla T }$	$\beta; u; v; w; \vec{U}; \nabla T$	Equation 6
$M = \sum \vec{U} \nabla T / N$	$\vec{U}; \nabla T; N$	Equation 7
$\beta_m = \frac{\sum \beta_{i,j,k} d^{i,j,k}}{\sum d^{i,j,k}}$	$\beta_m; c_p; v_{i,j,k}$	Equation 8
$\lambda_{FSP} = \frac{\sum_{\cos \beta_i \leq 1} \cos \beta_i}{\sum_{\cos \beta_i \leq 1} \cos \beta_i} \times 100\%$	$\beta; \lambda_{FSP}$	Equation 9
$\oint \Omega \rho c_p (\vec{U} \cdot \nabla T) d\Omega = \oint_w k \frac{\partial T}{\partial y} dS = q_w$	$\rho; \vec{U}; \nabla T; \Omega; k; q_w$	Equation 10
$\int_0^1 (\vec{U} \cdot \nabla \vec{T}) d\bar{y} = \frac{Nu_x}{Re_x Pr} = Fc$	$\vec{U}; \nabla T; Nu; Re; Pr; Fc$	Equation 11
$\vec{U} \cdot \nabla C = D \nabla^2 C$	$\vec{U}; D; \nabla C$	Equation 12
$Sh = Re Sc \int_0^{\delta_{m/l}} (\vec{U} \cdot \nabla \vec{C}) dY$	$Sh; Re; Sc; \delta_{m/l}; \vec{U}; \nabla \vec{C}$	Equation 13
$\alpha = \arccos \frac{\vec{U} \cdot \nabla C}{ \vec{U} \nabla C }$	$\alpha; \vec{U}; \nabla C$	Equation 14
$\vec{U} \cdot \nabla p = \xi \nabla^2 p$	$\nabla p; \vec{U}; \xi$	Equation 15
$Eu = Re Li \int_0^1 \int_0^1 -[\vec{U} \cdot (-\nabla \vec{p})] dXdY$	$Eu; Li; Re; \vec{U}; \nabla p$	Equation 16
$\theta = \arccos \frac{\vec{U} \cdot (-\nabla p)}{ \vec{U} -\nabla p }$	$\theta; \vec{U}; \nabla p$	Equation 17
$P\vec{U} \cdot \nabla \vec{U} = -\nabla P + \nabla \cdot (\mu \nabla \vec{U}) + (\frac{\rho}{2C_\Phi} A_0 \nabla Y + \rho \vec{U} \cdot \nabla \vec{U})$	$C_\Phi; P; \vec{U}; A_0; \rho; Y$	Equation 18
$\int_0^{\delta_{hx}} (\vec{U} \cdot \nabla H_v \cos \alpha_h) dy = -\lambda \frac{\partial T}{\partial y} _{w} + N_y c_p T_w = q_w$	$\delta_{H,x}; \vec{U}; \alpha_h; \nabla H_v; \lambda; T; N_y; c_p; q_w$	Equation 19
$\gamma = \arccos \frac{\nabla T \cdot \nabla C}{ \nabla T \nabla C }$	$\gamma; \nabla C$	Equation 20
$-\vec{U} \cdot \nabla p = -\vec{U} \nabla p \cos \theta$	$\theta; \nabla p; \vec{U}$	Equation 21
$Fc = \frac{Nu_x}{Re_x Pr} = \int_0^1 (\vec{U} \cdot \nabla \vec{T}) d\bar{y}$	Fc	Equation 22

In practical engineering applications, the process of convective mass transfer is often accompanied by energy conversion. Therefore, in the study of convective mass transfer, heat transfer also occurs at the same time, and the coupling mechanism of its interaction also affects the strengthening effect. Wu [13] deduced the synergy field equation (Eq. 19) of heat and mass transfer for two-dimensional incompressible Newtonian fluids without considering viscous heat dissipation from the first law of thermodynamics, the law of conservation of mass, the law of conservation of energy and the continuity equation; Sun [27] pointed out that the heat and moisture transfer process is an interactive coupling process in the research on the field synergistic analysis of the heat and moisture transfer process of the desiccant-coated heat exchanger, in addition to considering the synergistic effect between the velocity vector and the temperature gradient, and the synergistic effect between the velocity vector and the moisture gradient, the synergistic effect between the temperature gradient and the moisture gradient should also be considered, and on this basis, the synergy angle γ (Eq. 20) between the temperature gradient and the moisture gradient is proposed.

The field synergy theory is not only applicable to the transfer of heat and mass but also to the study of the propagation process of sound waves. Cao [48] expressed the synergy between the flow field and the sound field as the synergy between the velocity field and the pressure gradient field during the study of the flow noise mechanism propagation of the shell-and-tube heat exchanger and established the synergy equation (Eq. 21) and the formula of the synergy angle.

The field synergy angle and the field synergy number are used as the evaluation indexes of the synergy effect. The smaller the synergy angle is, the better the synergy effect will be. When considering the whole heat transfer process, the field synergy number (Eq. 22) is used to evaluate the heat transfer synergy effect [49]: when $Fc = 1$, that is $Nu_x = Re_x Pr$, the synergy effect is the best, but for the actual single-phase heat transfer process, Fc is much less than 1, indicating that there is a huge room for improvement in enhanced heat exchange. The equations of the field synergy theory are shown in Table 1.

With the deepening of field synergy research, its theories have become more and more mature, the research objects have ranged from ideal laminar fluids [7, 8, 11, 50] to more general turbulent fluids [14], the basis for theoretical research has transferred from the energy control equations [11, 13] such as thermal energy conservation [7] to the multi-theoretical thinking such as the variational principle [44], and the evaluation criteria of the field synergy effect is range from the average field synergy angle [11, 13] to the field synergy number [14]. At the same time,

the area of field synergy is not only limited to the study of convective enhanced heat transfer, but also extends to the research of convective mass transfer and heat-mass synergy, and has achieved certain results, proving the applicability and the maturity of the field synergy theory.

Application of field synergy

Based on the proposal and development of field synergy, the theory of field synergy is becoming more and more perfect and mature. Many scholars have applied the theory to engineering practice based on research on the theory and achieved fruitful results.

Heat exchanger

The application of field synergy theory in heat exchangers mainly improves the synergy of velocity field and temperature gradient field by changing the structure of channels and fins, and adjusting the shape and number of fins. In addition, the heat exchanger can also be combined with a desiccant to improve the efficiency of heat and mass transfer.

Channel structure

Heat exchangers have widely used components in production and living areas, and improving their heat exchange efficiency is an important content of scholars' dedicated research [51, 52]. Besides improving the heat transfer performance of the heat exchanger, it is also necessary to consider factors such as saving manufacturing costs, saving structural space, and reducing pumping power [17]. The field synergy theory can improve its heat transfer performance by improving the synergy between parameters without changing the original boundary conditions. The research on improving the performance of heat exchanger pipes by using the theory of field synergy has been relatively common and mature, mainly reflected in corrugated pipes [11], circular pipes [14, 44, 53–55], trapezoidal pipes [19], cosine pipes [20], fin pipes [13, 23, 24, 56], shell pipes [57, 58], elliptical pipes [59], rotating pipes [55], cavity-ribbed pipes [45], and so on.

Hamid [59] analyzed the heat exchange performance of heat exchangers with circular and elliptical tubes based on the theory of field synergy in the study of seawater desalination devices using solar-assisted multi-effect distillation. The average synergy angle of the elliptical tube is smaller than that of the circular tube, and the average synergy number and heat transfer rate are increased by 22.68% and 35.98%, respectively. Kuo [19] conducted a numerical simulation study on a heat exchanger with a trapezoidal tube structure

to evaluate its fluid flow characteristics and heat transfer performance, the result indicated that the trapezoidal tube structure can improve the field synergy between the velocity vector and the temperature gradient, thereby enhancing the heat transfer effect. Zhang [20] studied the heat transfer performance of cosine tube heat exchangers and analyzed the effect of different amplitudes on the heat transfer performance according to the theory of field synergy. The smaller the amplitude is, the smaller the average of the field synergy angle will be, which can lead to better field synergy and a higher heat transfer capacity. Zhai [45] studied the synergistic optimization of secondary flow and heat transfer in cavity-ribbed double-layer microchannels with three different cross-sections, indicating that the geometric design of layered microchannels must consider the synergistic effect of temperature field and velocity field. The research on different types of heat exchanger pipes has yielded fruitful results, in view of this, the principle of field synergy can be used to guide the design of heat transfer units and heat exchangers [11, 12, 60], including improving the structure and shape of pipe fittings [34, 44], thus inducing multiple longitudinal vortices [61], and then promote the research and optimal design of vortex generators [56, 62], and eventually improve the heat exchange efficiency of the heat exchanger.

Fin structure

The structural design of heat exchangers is not only reflected in the selection and optimization of heat exchanger pipes but also related to the design of the fins [63]. By analyzing the synergistic effect of the fluid velocity field and the temperature gradient field under the different structural forms of the fins, we can seek the optimal design with the best synergy effect.

The optimal design of the fin structure of the heat exchanger is mainly reflected in the selection and arrangement of the number, position, and shape of the fins [22–26], and then selected the optimal combination with the highest synergistic efficiency. He [64] established a three-dimensional numerical model to study the effect of the five factors of Reynolds number, fin spacing, tube row number, transverse and longitudinal tube spacing on the laminar flow thermal exchange and fluid flow characteristics of plate fin-tube heat exchangers and analyzed the results from the perspective of field synergy. With the increase of Re , the average synergy angle increases, and the synergy between velocity and temperature gradient weakens. When the fin spacing is 0.6 mm, the average synergy angle is the smallest, that is, the synergistic effect between velocity and temperature gradient is the best. This result is consistent with the field synergy theory. At the same time, the field synergy angle increases with the increase of the number of tube rows, so when the flow rate is constant, increasing the number of

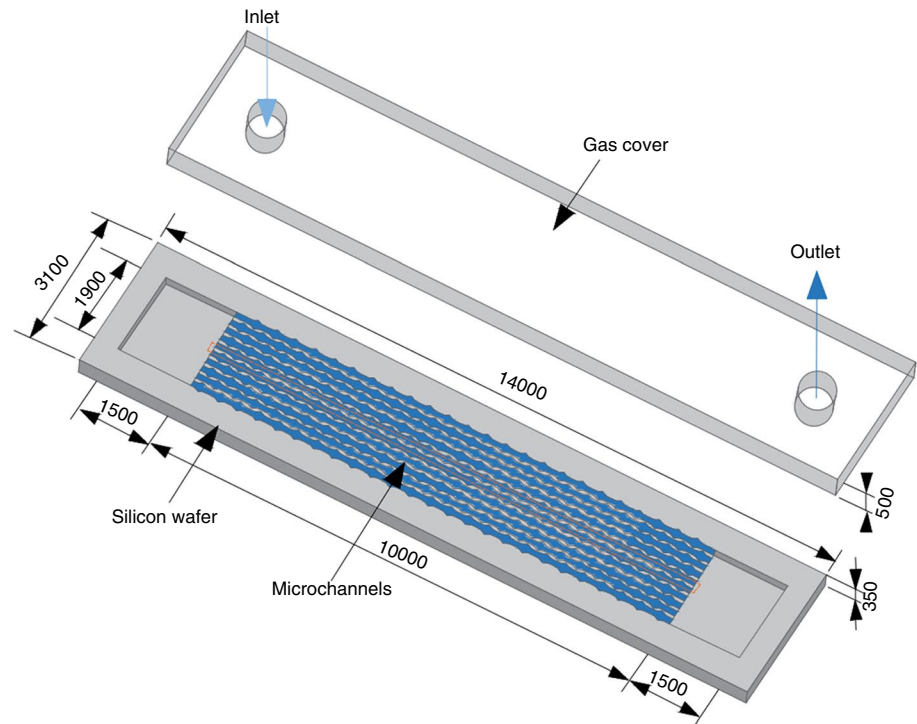
tube sections can reduce the synergistic effect of the fluid velocity field and the temperature gradient field. Important progress has also been made in the morphological design of heat exchanger fins, such as the use of flat fins composed of continuous metal sheets, corrugated fins that generate streamlined pipes by bending the base plate [65], slotted fins with raised strips [56, 61, 62, 66, 67], shutter fins, triangular fins [68], sawtooth fins [69], punched fins [70], outer fins [55, 71], special fins [72, 73], H-fins and composite fins [74, 75]. Mehra [76] studied three different types of finned heat exchangers, and analyzed and evaluated their heat transfer performance according to the theory of field synergistic heat transfer enhancement, the heat exchanger structure with the best synergy effect can improve its 7% of heat transfer performance., while saving 14.4% of aluminum sheet usage, which greatly saves costs.

The combination of channels and fins

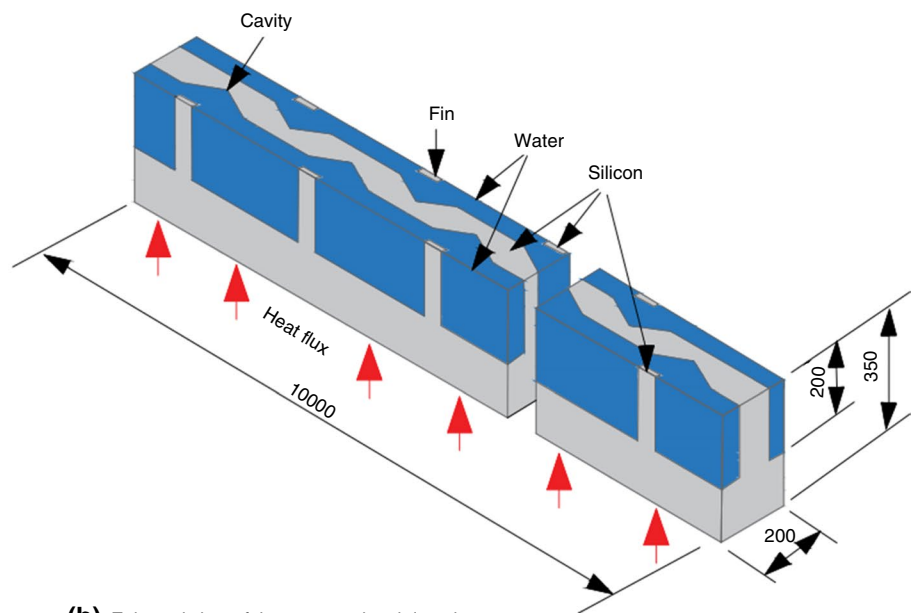
In the first two sections, the channels and fins were optimized separately, and the optimization design study of the combination of the channels and fins was also started, and people began to seek the possibility of triple effect from a comprehensive perspective. For the integrated design of the combination of channels and fins, it is more common in micro-heat sinks, which are widely used in the design of microelectronic devices and chips [36]. The research on micro-radiators mainly includes arranging fins in the center of microchannels with cavities, which aims to study their heat transfer performance [7, 8, 14]. From the perspective of field synergy, using the synergistic relationship between the fluid velocity field and the temperature gradient field can evaluate the performance of micro-components [11, 12, 36, 60, 77]. Li [78] applied the field synergy theory to the study of a new type of micro-channel radiator with the combination of the cavity and fin, which provided a new idea and method for the development of the radiator.

Whether a single-phase flow [79] or a converging flow channel [80] such as non-Newtonian fluids [81], the heat transfer in the cavity is affected by microscale effects [82]. To optimize the design of the combination of the cavity and fin from the perspective of field synergy and seek the best heat transfer effect, Li [78] designed a new type of micro-channel heat radiator (Fig. 3), due to the symmetry characteristics and to simplify the simulation, the part marked in the orange dotted box in the figure is selected for simulation research. The isosceles triangular cavity microchannels with four different fins, namely rectangular, streamlined, rear descending fin, and front descending fin, are numerically simulated and studied, and an unobstructed conventional channel is selected for comparison. The channel structure diagram is shown in Fig. 4, among which four micro-complex channels are isosceles triangle cavity rectangular fin

Fig. 3 Structure diagram heat radiator [78]



(a) Schematic diagram of a microchannel heat radiator



(b) Enlarged view of the computational domain

(ITC-RF), isosceles triangle cavity streamlined fin (ITC-SF), isosceles triangle cavity posterior fall fin (ITC-BDF), isosceles triangle cavity front fall fin (ITC-FDF).

The fluid flow and heat transfer of four new microchannel heat radiators with the combination of the cavities and fins were studied by applying the theory of field synergy in the range of Re from 173 to 635. Figure 5 reflects the variation of the synergy angle β between the fluid velocity

field and the temperature gradient field of different types of microchannels at different flow rates. Compared with the traditional barrier-free channel, the synergy angle of the new microchannel structure is significantly reduced. According to the Eq. (2), Eq. (3), the smaller the β is, the smaller effect of the synergy between the velocity field and the temperature field will be, that is, the synergistic effect of the new microchannel structure is better than that of the traditional

Fig. 4 Structure diagram of different types of microchannels [78]

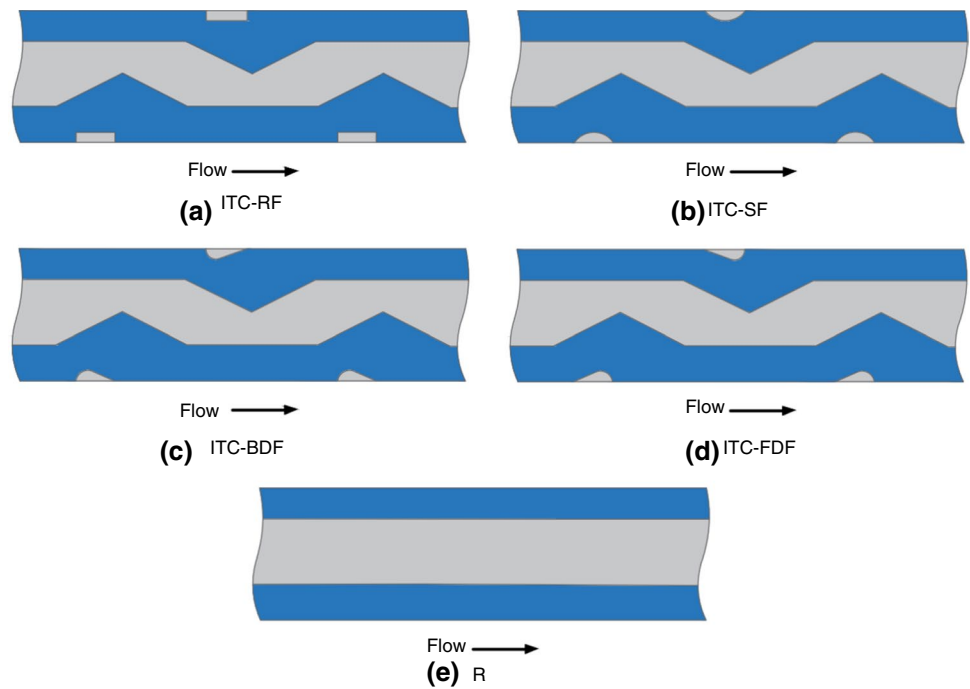
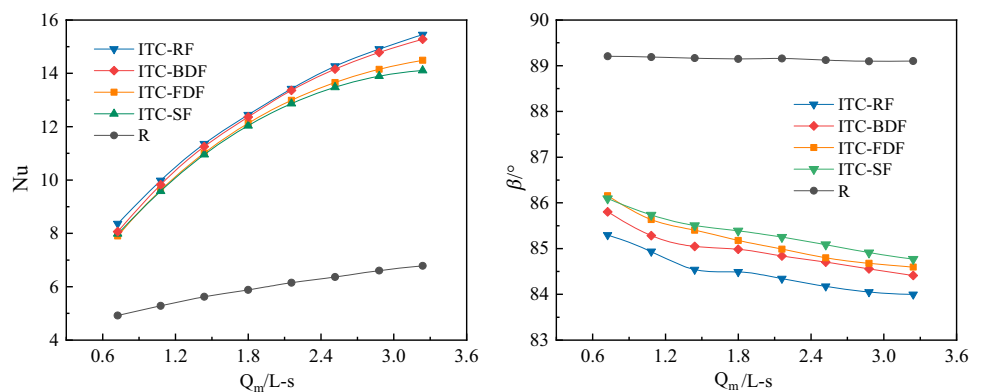


Fig. 5 Variation of Nu and β with volume flow in different microchannels [78]



structure, which is more conducive to enhancing convective heat transfer. At the same time, among the four new microchannel structures, the synergy angle of the ITC-RF microchannel is the smallest, indicating that the rectangular fin is the microchannel structure that is most conducive to promoting the synergy between the velocity field and the temperature gradient field, which is consistent with the graph of Nu in Fig. 5. The comparison graph of the number of field synergies in Fig. 6 better reflects the highest synergistic effect of the ITC-RF microchannel [78].

The combination with the heat exchanger and desiccant

Conventional heat exchangers [83] mainly play the role of enhancing convective heat transfer. Based on conventional heat exchangers, the surface is covered with desiccant, so that it has the dual functions of heat exchange

and dehumidification [84], and the desiccant-coated heat exchanger (DCHE) [85] was developed based on this principle. When the hot and humid air flows through the DCHE, in addition to the heat exchange of the heat exchanger and the dehumidification of the desiccant coating, the desiccant coating will generate adsorption heat when absorbing water vapor, which is taken away by the cold fluid of the heat exchanger, so DCHE is a coupled process of heat and mass transfer [27]. To study its coupling process, many scholars have improved its heat and mass transfer capacity by establishing mathematical models to analyze its characteristics [86–89], changing desiccant materials [1, 90–95], and changing heat exchanger types [94, 95]. And they also use the field synergy theory to guide the design of DCHE, as a result, its structure size is optimized [27].

Based on the theory of heat and mass field synergy, Li [27] explored the effect of different fin pitches on the heat

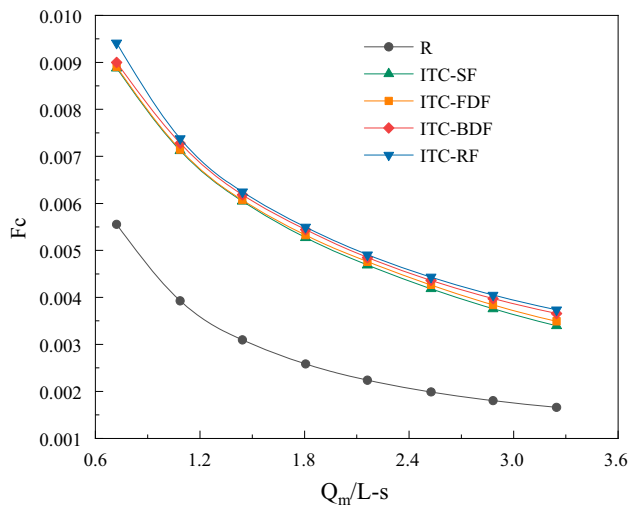


Fig. 6 Variation curve of the field synergy number with volume flow in different microchannels [78]

and moisture transfer process and obtained the optimal design. Under the condition that other parameters remain unchanged, five models with different fin pitches are selected as shown in Table 2. In the research on the synergistic effect of heat and mass transfer fields, the smaller the synergy angle is, the better the synergy effect will be, and the more conducive to improving the heat and mass transfer. From the synergy angle curves of 5 different fin pitches (Figs. 7, 8), the synergy angle of different processes was compared and

analyzed. Under the condition of constant fin length, width, number, and coating quality. The smaller the field synergy angle is, the higher the cooling (sensible cooling) ability in the dehumidification process will be, which also leads to a better effect on the dehumidification. And in the regeneration process, with the increase of the fin pitches, the field synergy angle becomes larger, and the sensible heat capacity also becomes lower. Therefore, it should be considered that the actual engineering needs to design the DFHE. If it is a refrigeration and dehumidification function in summer, a DFHE with a larger fin pitch should be designed, while a DFHE with a smaller fin pitch should be used in winter to improve its heating and humidifying effect.

The previous research on enhanced heat transfer based on the field synergy theory mainly analyzed the average field synergy angle of the entire heat exchanger to evaluate its overall heat transfer effect, but it could not evaluate the local heat transfer effect. Based on this limitation, some scholars carried out research on the local heat transfer effect and the local field synergy angle and got some progress. Habchi [74] analyzed the synergistic effect of the local synergy angle when studied vortex generators with different structures of turbulent fluids; Zhu [96] analyzed the local Nu number and the local synergy angle of the laminar and turbulent flow between two parallel plates and concluded that the field synergy theory can be used to analyze the local Nu number. Mehra [17] studied the effect of local field synergy on heat transfer performance by changing the structure of flat fins and found a new flat fin structure that can save 14.4% of

Table 2 The structure size parameters of five DFHEs [27]

Parameters	Length of the fins/m	Depth of the fins/m	Width of the fins/m	Layer number of fins/m	Fin pitches/m
DFHE 1	0.3	0.044	0.214	0.142	1.184
DFHE 2	0.3	0.044	0.258	0.142	0.994
DFHE 3	0.3	0.044	0.3	0.142	0.863
DFHE 4	0.3	0.044	0.342	0.142	0.765
DFHE 5	0.3	0.044	0.386	0.142	0.685

Fig. 7 Variation curve of synergy angle of velocity field and temperature gradient field with different fin pitches in dehumidification and regeneration process [27]

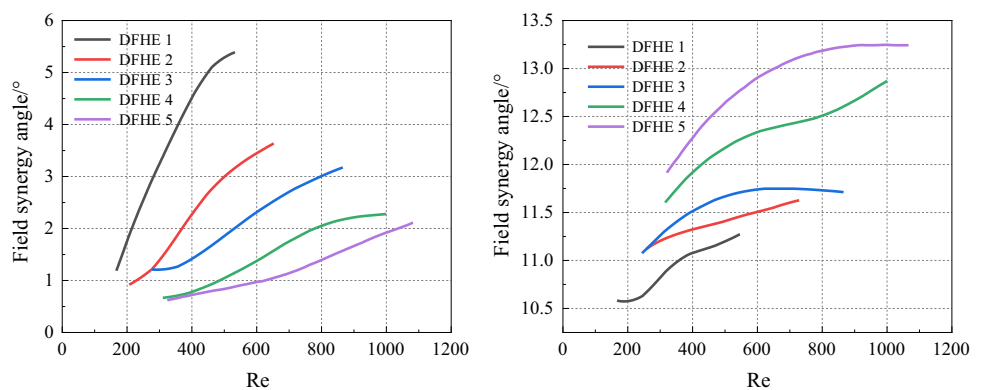
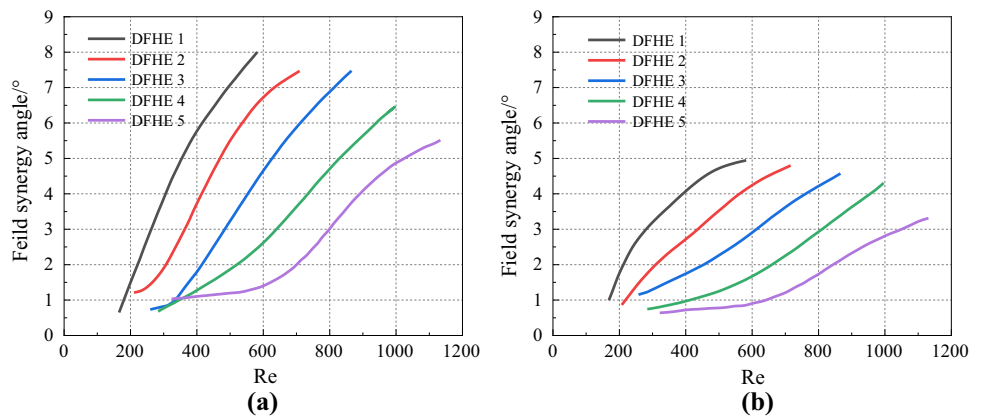


Fig. 8 Synergy angle of humidity gradient field and velocity field (a), and synergy angle of humidity field and temperature gradient field (b) with different wing pitches in the dehumidification process [27]



aluminum material and improve heat transfer performance by 7%.

The field synergy theory is not only applicable to the study of heat transfer performance of heat exchangers but also to the study of sound energy transmission. Cao [48] used the theory of field synergy to study the noise propagation process of shell-and-tube heat exchangers. By establishing the flow field and pressure gradient field which reflect its propagation performance, they concluded that improving the synergy of the flow field and the sound field can increase the exchange of acoustic energy between the fluid and the wall.

Closed wet cooling tower

The closed wet cooling tower (CWCT) is a cooling system widely used in the chemical industry, construction, metallurgy, and other fields [97]. Many scholars have carried out a lot of research to improve its cooling heat transfer performance and water-saving performance. Xie [37] carried out numerical simulations of CWCT with different fin-tube structures to analyze the influence of parameters such as inlet air angle on heat and mass transfer by using multi-field synergy theory and obtained the conclusion that the increase in the degree of synergy between the velocity field, temperature field and humidity field can enhance the heat and mass transfer. The heat and mass transfer performance of a CWCT is expressed by the heat transfer coefficient χ (Eq. 23) and the mass transfer coefficient ζ (Eq. 24):

$$\chi = \frac{m_a c_{pa}}{S} \ln \left(\frac{T_w - T_{a,in}}{T_w - T_{a,out}} \right) \quad (23)$$

where, m_a is the mass flow of dry air, kg s^{-1} ; T is the temperature, K.

$$\zeta = \frac{m_a}{S} \ln \left(\frac{i'_w - i_{a,in}}{i'_w - i_{a,out}} \right) \quad (24)$$

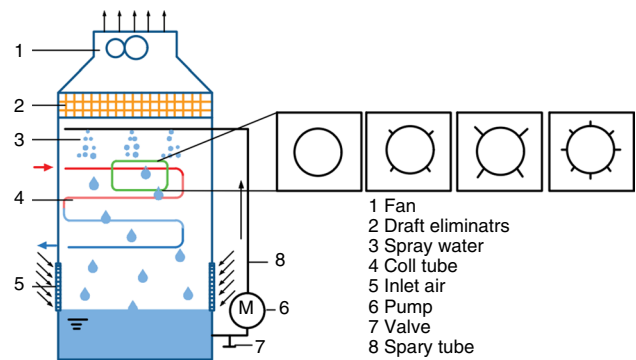


Fig. 9 Schematic diagram of the closed wet cooling tower [37]

where, i_a is the enthalpy of the air, J; and S is the heat or mass transfer area, m^2 .

Xie [37] carried out the numerical simulation of the closed wet cooling tower model (Fig. 9) and obtained the change curves of humidity difference, heat transfer coefficient and mass transfer coefficient with the angle of intake air (Fig. 10). When the intake angle is from 30° to 45° , the humidity difference, heat transfer coefficient and mass transfer all show an upward trend. When the temperature exceeds 45° , the parameters all decrease with the increase of the intake angle, indicating that the performance of CWCT is the best when the intake angle is 45° . In addition, the heat transfer coefficient and the mass transfer coefficient of the finned tube are higher than those of the ordinary tube. When the intake angle is 45° , the finned tube structure is about 75% higher than the ordinary tube structure. This is since when the inlet air angle increases from 30° to 45° , the synergy gradually increases with the decrease of the synergy angle. When the synergy angle is 45° , the heat transfer coefficient and mass transfer coefficient are about 1.15 and 1.5 times that of 30° , respectively.

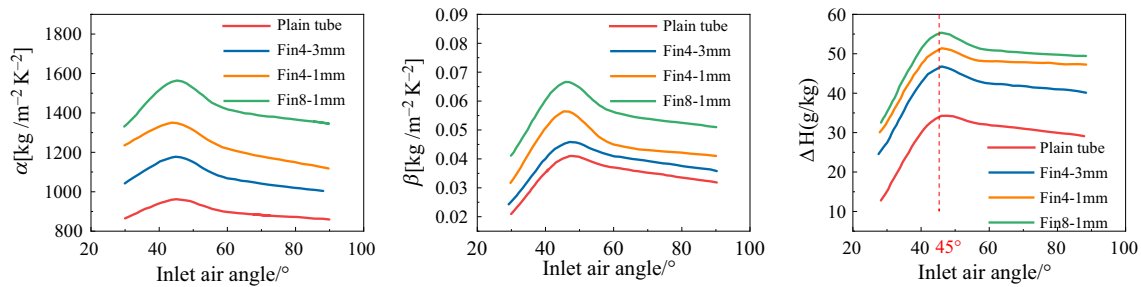


Fig. 10 Influences of inlet air angle on **a** humidity difference (ΔH), **b** air–water mass transfer coefficient β , and **c** heat transfer coefficient α [37]

Combustion reactor

Based on the theory of field synergy, Wang [98], Zeng [99] used numerical simulation to analyze the velocity field, temperature gradient field and the distribution of the field synergy angle of the advanced vortex combustor under different inflow velocity, inflow temperature, wall temperature and gas equivalence ratio. On the premise of considering the convective and radiative heat transfer losses, E [100] carried out the numerical simulation and field synergistic analysis of the finite reaction rate model and vortex crushing combustion model which established when methanol fuel is diffused in an alcohol-based fuel burner. Biomass pellet fuel has broad application prospects in the field of combustion reactors due to its high efficiency and environmental protection. Jia [29] carried out a numerical simulation of the biomass rotary combustion process and studied the performance of the biomass rotary burner and the influence of and excess air coefficient on the combustion effect of biomass rotary burner base on the field synergistic analysis.

Figure 11 is a schematic diagram of the structure of the biomass pellet rotary burner. With Chinese fir pellets as the biomass fuel, the combustion conditions of the biomass pellet burner under four working conditions of excess air coefficients of 1.0, 1.4, 1.8, and 2.4 are simulated. Through numerical simulation, the cosine distribution diagram of the angle between the velocity vector and the enthalpy gradient in the combustion chamber under the conditions of different excess air coefficients is obtained (Fig. 12). It can be seen from the figure that the temperature field changes accordingly due to the intensity of the combustion reaction which is changed with the increase of the excess air coefficient. The gas in the combustion chamber also changes due to the expansion degree of the combustion heat, which leads to the difference in the velocity field, as a result, causing the cosine distribution of the angle between the velocity vector and the enthalpy gradient in the combustion chamber to change with the excess air coefficient. When $|\cos \alpha| \geq 0.8$, the combustion performance of the biomass rotary burner is the best. According to the combustion calculation results (Table 3)

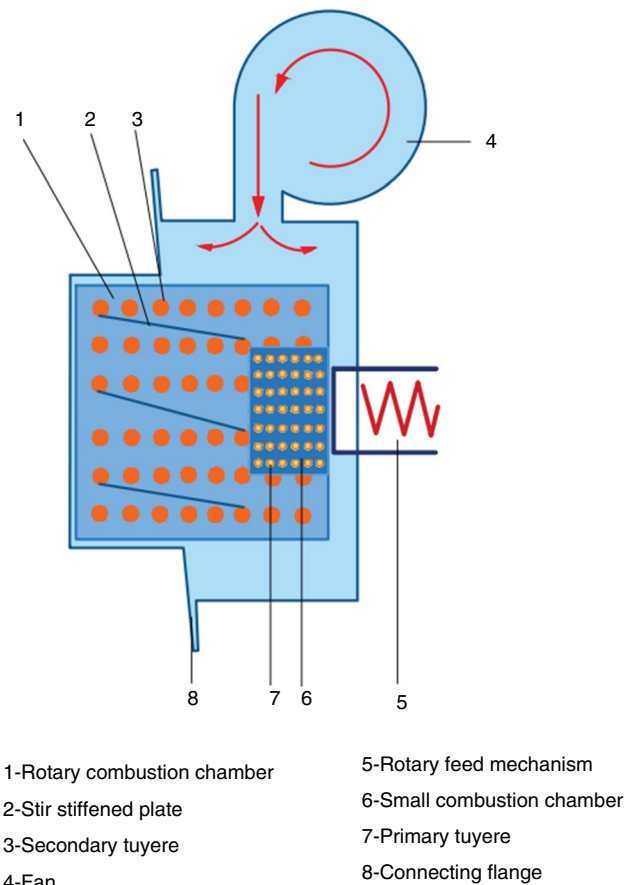


Fig. 11 Burner structure diagram [29]

and the distribution of the optimal area ratio (Fig. 13) under different excess air coefficients, the optimal combustion area of the biomass rotary burner combustion heat transfer process is at the excess air coefficient of about 1.2, and the proportion is 29.2%; the synergy effect between the velocity vector and the enthalpy gradient in the combustion heat transfer process of the biomass rotary burner is well, which reflects the highest combustion rate and highest combustion efficiency of the biomass rotary burner.

Fig. 12 Field synergistic cosine angle distribution diagram of the burner [29]

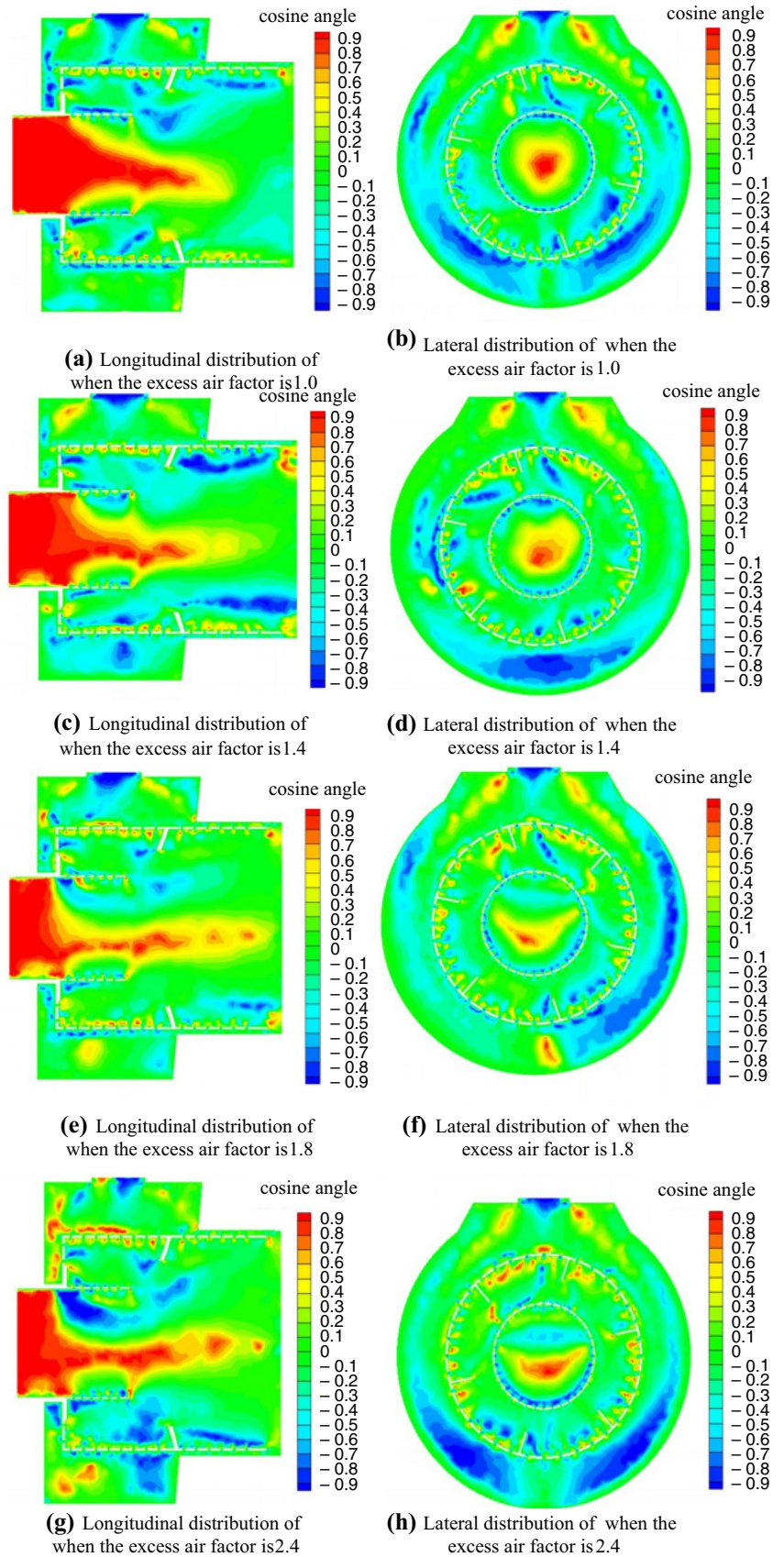


Table 3 Field Synergistic calculation results of combustion process of biomass rotary burner [29]

The excess air factor	Optimal area ratio / %	velocity / $m \cdot s^{-1}$	Temperature / K
1.0	8.5	0.418–0.836	636–1390
1.2	29.2	0.418–0.836	568–1520
1.4	15.9	0.620–1.510	826–1660
1.6	16.7	0.667–1.670	848–1740
1.8	18.2	0.749–1.870	851–1750
2.4	21.4	0.992–0	716–1770

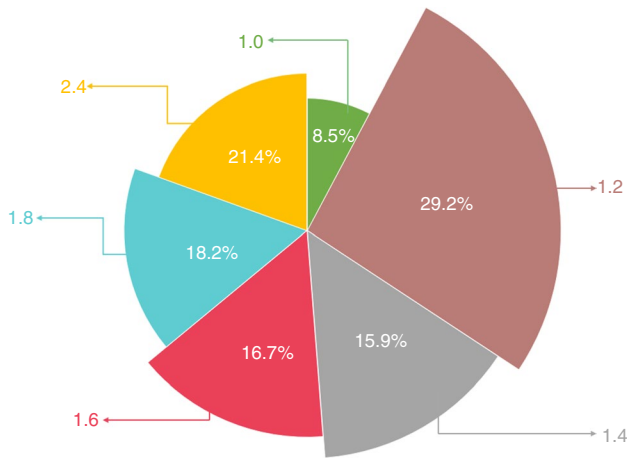


Fig. 13 Optimum ratio of combustion under different excess air coefficients

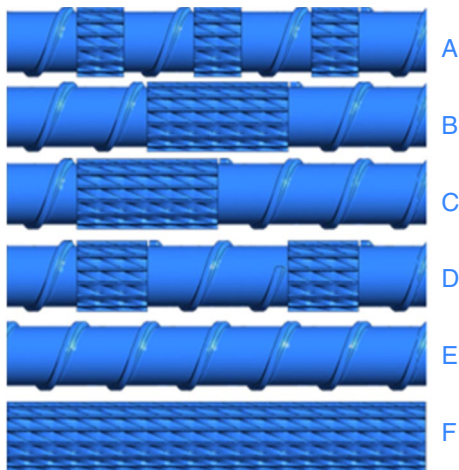


Fig. 14 Screw element structure diagram [33]

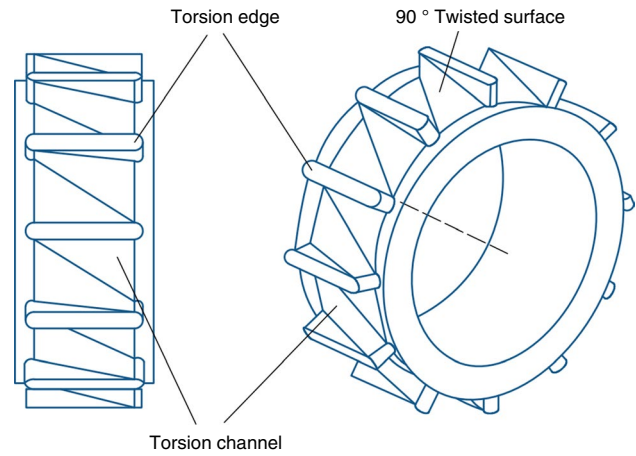


Fig. 15 The geometry diagram of the torsion element [33]

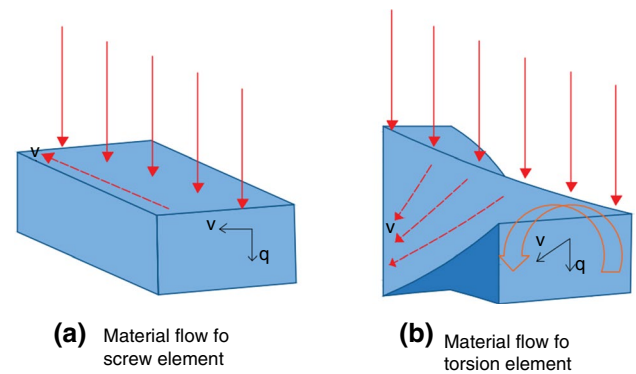


Fig. 16 Fluid flow models for screw elements and torsion elements [33]

Screw plasticizing system

The screw plasticizing system is a polymer plasticizing device used in extrusion, injection molding, and other processes. Optimizing the structure of the screw is extremely important to enhance the growth rate of the polymer and improve its product quality and production efficiency [101]. Jian [33] carried out numerical simulations of screw elements with different torsional structures and screw structures, respectively, and analyzed their heat transfer and flow characteristics based on the field synergy theory. Elements with torsional structures improved the synergy effect of temperature gradient and velocity vector, increased the Nusselt number and local heat transfer coefficient, which had better heat transfer performance.

Jian carried out numerical simulations of screw elements with six different structures from A to F (Fig. 14), where E is a pure screw structure element, F is a pure torsional structure element, and their geometric structure is shown in Fig. 15, A–D is the different arrangement of screw structure

Fig. 17 The variation curve of the average field synergy angle of velocity vector and temperature gradient and the Nu number with screw speed [33]

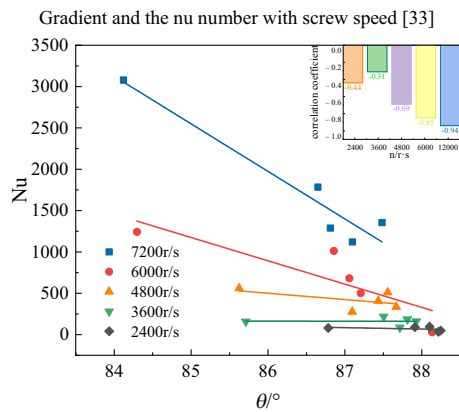
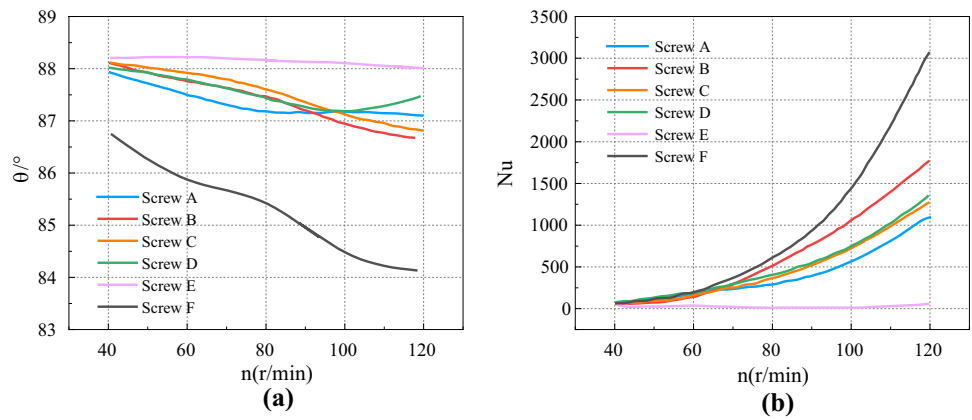


Fig. 18 Relationship between Nu number and field synergy angle (the inset is the Pearson correlation coefficient) [33]

and torsion structure, the screw structure and the torsion structure show different heat transfer characteristics due to their different fluid flow states (Fig. 16).

According to the change curve of the average field synergy angle with the screw speed (Fig. 17a), the synergy angle of structure E is the largest, indicating that the synergy between its velocity vector and gradient is the smallest, and the synergy angle of structure F is the smallest, which means the better synergistic effect of the speed vector and temperature gradient. The synergy angle of A-D showed a similar change trend, indicating that different arrangements have less effect on the synergistic effect. The variation curve of the Nu number in Fig. 17b shows the opposite characteristic of the synergy angle, so the correlation curve between the Nu number and synergy angle was drawn (Fig. 18) to explore the effect of synergy on convective heat transfer. It can be seen from the figure that the number of Nu decreases with the increase of the synergy angle, indicating that the larger the synergy angle is, the worse the synergy effect and the lower the heat transfer performance will be. According to the correlation coefficient diagram, when the screw speed is greater than 3600 r/s, the correlation coefficient increases

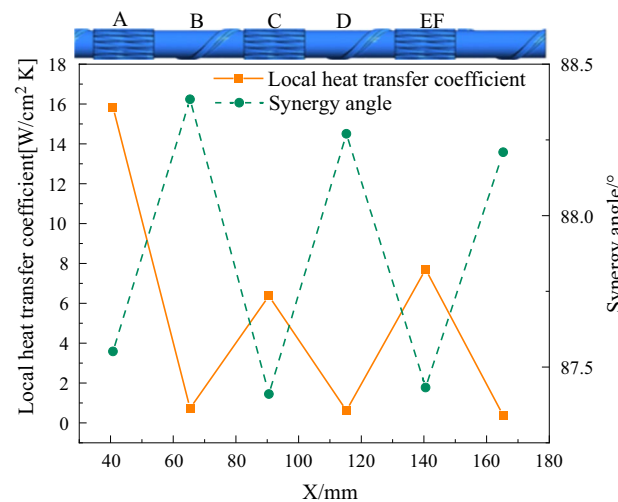


Fig. 19 The relationship between the local heat transfer coefficient and the local field synergy angle of the structure A when the rotation speed is 4800 r/s [33]

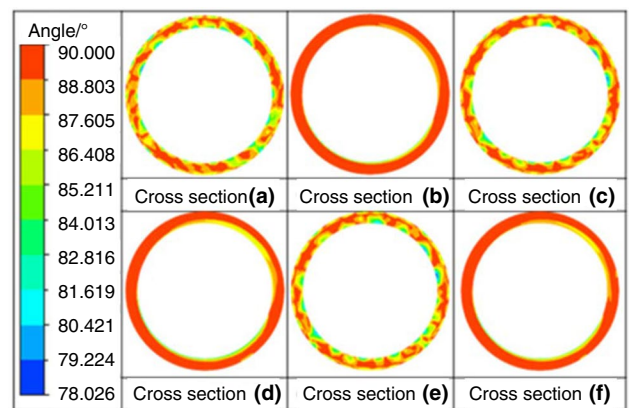


Fig. 20 Local synergistic angles of structure A at different sections when the rotational speed of 4800 r/s (a, b, c, d, e, f is the cross section of the structure)[33]

gradually with the rotation speed, and the increment of Nu is mainly from the size of the synergy angle, that is, the synergistic effect of the velocity field and the temperature gradient field.

To more intuitively express the effect of screw structure and torsional structure on heat transfer, the local field synergy angle and local heat transfer coefficient of structure A element with a screw speed of 4800 r/s were analyzed (Fig. 19). The torsional structure has a smaller synergy angle and a larger heat transfer coefficient than the screw structure, indicating that the synergistic effect of the torsional structure is better, which can enhance the heat transfer effect.

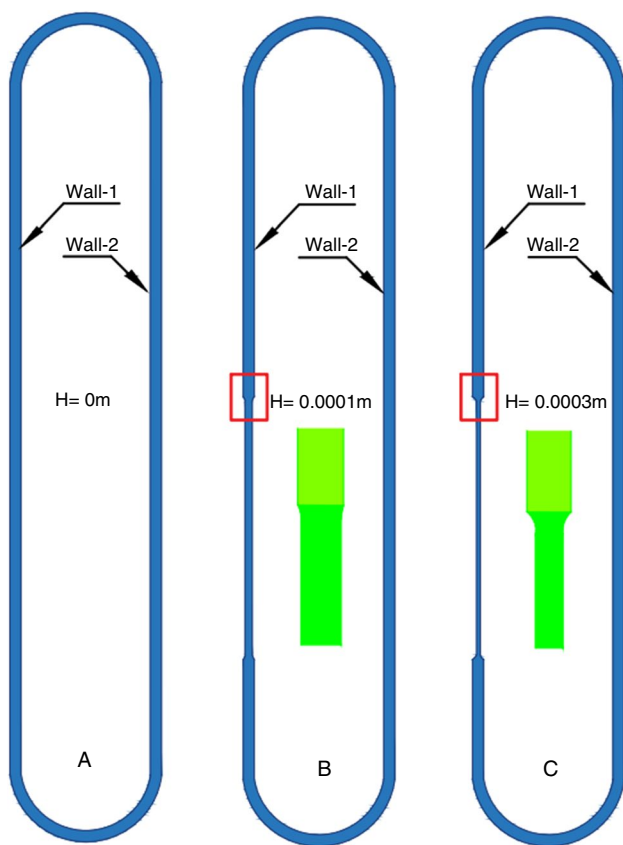


Fig. 21 Physical model diagram of COHP(A is the conventional structure, B and C are the new narrow tube structures) [34]

According to Fig. 20, from the distribution of synergy angles at different sections, it can be seen that at sections b, d, and f, that is, the screw structure, the local synergy angle is larger and the synergy effect is poor, and at the sections a, c, e, that is the torsion structure, the synergy angle is alternately arranged, and the synergy effect is better.

Closed oscillating heating tube

The closed oscillating heating tube (COHP) is widely used in solar collectors [102], drying systems [103–105], microelectronic components [106], and other fields [34] due to its simple structure and good heat transfer performance. COHP is composed of three parts: evaporation, adiabatic, and condensation, and its heat transfer process is completed through the phase transition of the fluid [34]. E [34] studied the heat transfer performance of COHP with a new narrow tube by numerical simulation and experiment method based on the field synergy theory. The model diagrams of the conventional tube and the new narrow tube COHP are shown in Fig. 21.

Based on the field synergy theory, the data results of three different models are obtained by numerical simulation, which is shown in Table 4. Model C has the best synergy effect, while the conventional COHP structure, that is, structure A has the worst synergy effect. From the synergistic effect diagram of the velocity field and temperature field of structures A and C (Fig. 22), it can be found that under the same other conditions, the temperature of structure A is generally higher than that of structure C, especially in region 2. And the velocity direction of structure A is more disordered, reflecting its poor synergy with the temperature gradient field. To explore the relationship between the field synergy effect and heat transfer performance, E [34] quoted the average heat transfer coefficient (Eqs. 25, 26) and Prandtl number (Eq. 27) which react to the heat transfer performance. From Fig. 23, the average heat transfer coefficient of structure C is 31.93% higher than that of structure A in wall-1 and is 26.37% higher in wall-2, the Prandtl number of structure C is also obvious higher than that of the A structure, indicating that the C structure has better heat transfer ability. The comprehensive analysis of the field synergy effect and the heat transfer ability show that improving the field synergy can improve the heat transfer ability, so structure C can be used to optimize the design of the COHP.

Table 4 Result of the field synergy calculation [34]

Model number	Synergy degree/%	Velocity/m\cdots	Maximum temperature of wall-1/K	Minimum temperature of wall-2/K
A	7.492	0.21–2.12	369.436	273.619
B	9.492	0.35–2.53	306.859	282.199
C	13.631	0.49–2.91	301.111	284.792

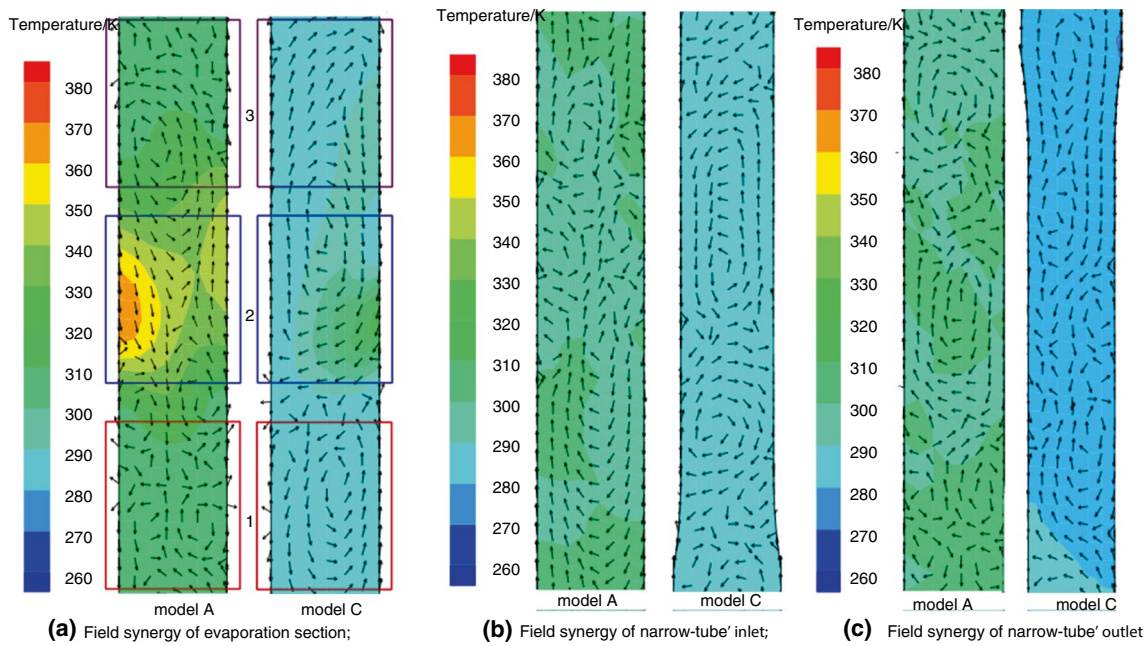
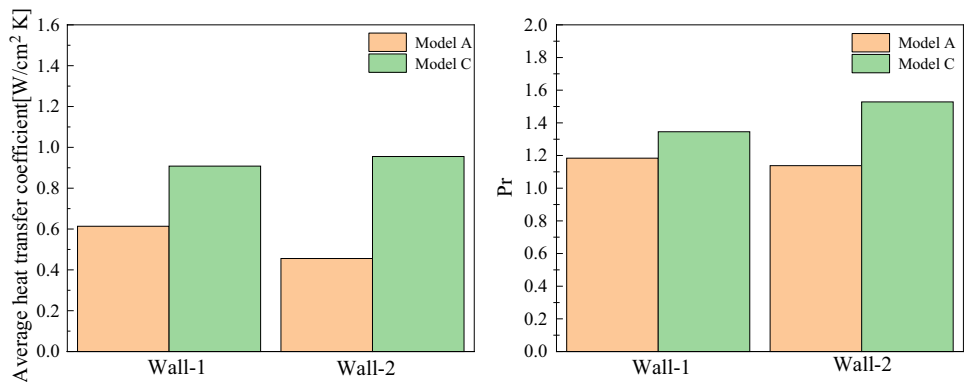


Fig. 22 The synergistic effect of velocity field and temperature field of structures A and C [34]

Fig. 23 Comparison of average heat transfer coefficients and Prandtl numbers for structures A and C [34]



$$h_{\text{eff1}} = \frac{\overline{Q}_{\text{wall-1}}}{\overline{T}_{\text{wall-1}} - T_{\text{ref1}}} \tag{25}$$

$$\text{Pr} = \frac{\overline{c_p \mu}}{k} \tag{27}$$

$$h_{\text{eff2}} = \frac{\overline{Q}_{\text{wall-2}}}{\overline{T}_{\text{wall-2}} - T_{\text{ref2}}} \tag{26}$$

where, $\overline{c_p}$ is the mean isobaric heat capacity, $\text{J}\cdot\text{kg}^{-1}\cdot\text{K}^{-1}$; $\overline{\mu}$ is the average dynamic viscosity, $\text{Pa}\cdot\text{s}$; k is the average thermal conductivity, $\text{W}\cdot\text{m}^{-1}\cdot\text{K}^{-1}$.

where, h_{eff1} is the heat transfer coefficient of wall-1, $\text{W}\cdot\text{m}^{-2}\cdot\text{K}^{-1}$; h_{eff2} is the heat transfer coefficient of wall-2, $\text{W}\cdot\text{m}^{-2}\cdot\text{K}^{-1}$; $\overline{Q}_{\text{wall-1}}$ is the average heat transfer of wall-1, J ; $\overline{Q}_{\text{wall-2}}$ is the average heat transfer of wall-2, J ; $\overline{T}_{\text{wall-1}}$ is the average temperature of wall-1, K ; $\overline{T}_{\text{wall-2}}$ is the average temperature of wall-2, K ; T_{ref1} is the reference temperature for evaporation section, K ; T_{ref2} is the reference temperature for condensing section, K .

Other fields

In the process of enhancing heat transfer, nanoparticles have a wide range of applications due to their special properties [107–114], and the research on nanofluids mainly focuses on turbulent flow characteristics and enhanced heat transfer mechanisms [115–122]. Yang [123] studied the heat transfer of Cu nanofluids with volume fractions of 0.25%, 0.5%, 1.0% and 2.0% at Reynolds numbers of 200, 250, and 300

according to the theory of field synergy, and concluded that when Re is 300 and the volume fraction of Cu is 2.0%, the effect of the heat transfer is the best, and the maximum heat transfer enhancement efficiency is 30%; Cui [124] simulated the enhanced heat transfer mechanism of nanoparticles with different mass fractions. As the mass fraction of nanoparticles increases, the field synergy angle decreases, and the synergistic effect becomes better. Long [32] analyzed the ion selectivity based on the synergy parameter in the analysis of the energy harvesting to enhance salinity gradients in the nanofluid reverse electro dialysis system. The results showed that the nano-blocker can significantly improve ion selectivity, increase membrane potential, and thus improve electrical energy and energy conversion efficiency. Among them, the power and energy conversion efficiency of 3.5×10^{-9} m nano-blockers are 100 times higher than that of traditional nanochannels, which can be increased by 362% and 1603.4%.

In addition to applications in heat exchangers, CWCT reactors, combustion reactors, etc., field synergy is also used in polysilicon chemical vapor deposition reactors (CVD) [38], photocatalytic oxidation reactors (POC) [35] heat and mass transfer analysis. An [38] used the field synergy theory to study the local heat and mass transfer performance of polysilicon chemical vapor deposition reactors with different channel configurations, the trapezoidal and wavy channel structures had a smaller synergistic angle between the velocity vector and temperature gradient, and the smaller synergy angle between the velocity vector and concentration gradient, which showed better heat transfer and mass transfer performance, so trapezoidal and wavy channels can be considered in the optimal design of silicon CVD reactors. Catalytic oxidation technology using ultraviolet radiation can reduce indoor pollutant concentrations and improve health problems, which has the advantages of both innovation and practicality [35, 50, 125–128]. The field synergy theory can optimize and analyze the photocatalytic oxidation reactor (POC) [35], improve the removal efficiency of pollutants and realize the enhancement of convective mass transfer [67]. Chen [35] deduced the field synergy equation of the photocatalytic oxidation reactor under specific boundary conditions. By solving the equation, the optimal velocity field with a high mass transfer rate can be obtained, it is proved by the numerical method that generating multiple longitudinal vortices in the plate reactor can enhance the mass transfer effect of laminar flow, and developed a new type of reinforced inner fin-discrete double diagonal rib plate (Fig. 24), with 9 pairs of diagonal fins along the

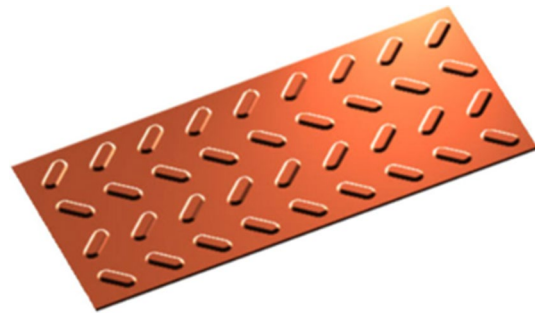


Fig. 24 The discrete double-inclined ribs plate [35]

fluid flow direction while 2 pairs perpendicular to the fluid flow. Through the numerical simulation of the diagonal rib, a longitudinal vortex is generated near the diagonal rib, which enhances the synergistic effect between the velocity field and the pollutant concentration gradient field.

With the development and maturity of the field synergy theory, its research has become more complete, and it has also been explored and applied in more and more fields. Its application in fluid flow drag reduction [129] has improved the fluid flow efficiency. The field synergy theory is also widely used in seawater desalination process [36], silica gel regeneration process [130, 131], heat pump system [132], thermoelectric system [133], electric vehicle [134, 135], diesel engine [136, 137], solar energy system [138], fuel cells [26], porous media [28], and so on. By establishing a dynamic three-dimensional computational fluid dynamics model, Li [36] conducted a field synergistic analysis of the heat and mass transfer system of the adsorption desalination cooling system and studied the synergy angle which expressed the heat transfer and the synergistic effect of the flow resistance and the adsorption driving force. It is found that the smaller the synergy angle is, the better the adsorption performance will be; when analyzing the output power combined system of the diesel engine [136, 137], the maximum increase of the optimized diesel engine is 6.5%, and the maximum braking specific fuel consumption is reduced by 6.1%. The field synergy theory can also guide the optimal design of diesel particulate filters [64, 70, 71, 76] and the fuel cells [26]. By optimizing the design of fuel cells [26], the influence of square and trapezoidal ducts was explored [65], and a new type of wavy airflow duct was designed [139]. Zhao [28] conducted experiments on the heat transfer process of porous media and analyzed their heat transfer performance based on field synergy (Fig. 25).

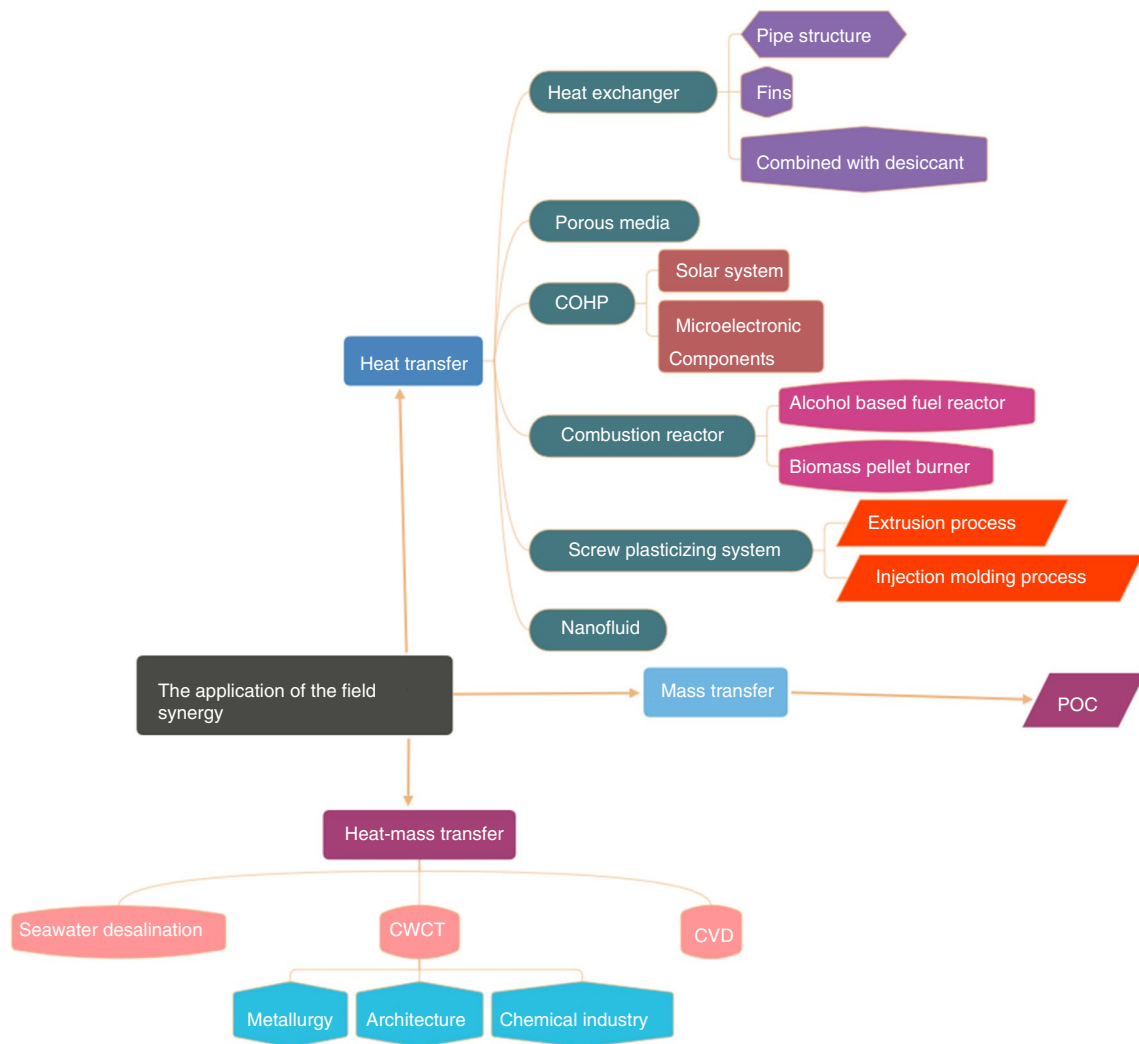


Fig. 25 is a summary diagram of the application of the field synergy

Analysis and application of field synergy theory in the cooling exchanger

Application background of cooling exchanger

In recent years, shallow coal mine resources have been continuously excavated due to the continuous increase in the demand for coal resources, and the coal mining work has continued to penetrate deeper into the ground. The continuous increase of mining depth, the rising of original ground temperature and the increasing of underground seepage have led to the increasingly prominent problem of heat and humidity in mines, which constantly threatens the health of workers and the development of mining work [39–42]. According to the survey, the accident rate of the working face at 303–310 K is 1.3–2.3 times higher than that of the working face below 303 K [140]. When the working environment temperature exceeds 305 K, it is considered a

high-temperature working environment, and when the relative humidity exceeds 60%, it is considered a high-humidity environment [141]. As shown in Table 5, more and more coal mines suffer from the damage of high temperature and humidity [142–145].

Heat damage in mine depends not only on the conditions of the rock mass itself [146, 147], such as thermal conductivity, internal rock gaps, and water content in the rock mass, but also on the mine ventilation equipment [148–150], such as the location and the parameter settings of fans and air ducts, and at the same time, the underground humid and hot air environment [82, 151], the heat dissipation of electrical and mechanical infrastructure [152], the oxidation of transported ores [153], and the self-compression heat of the underground air flow [154] can also have an impact on the environment. Research on the damp-heat environment in mines and mastering its damp-heat theory are crucial for

Fig. 26 Schematic diagram of heat and moisture exchange between a wet surrounding rock and wind flow

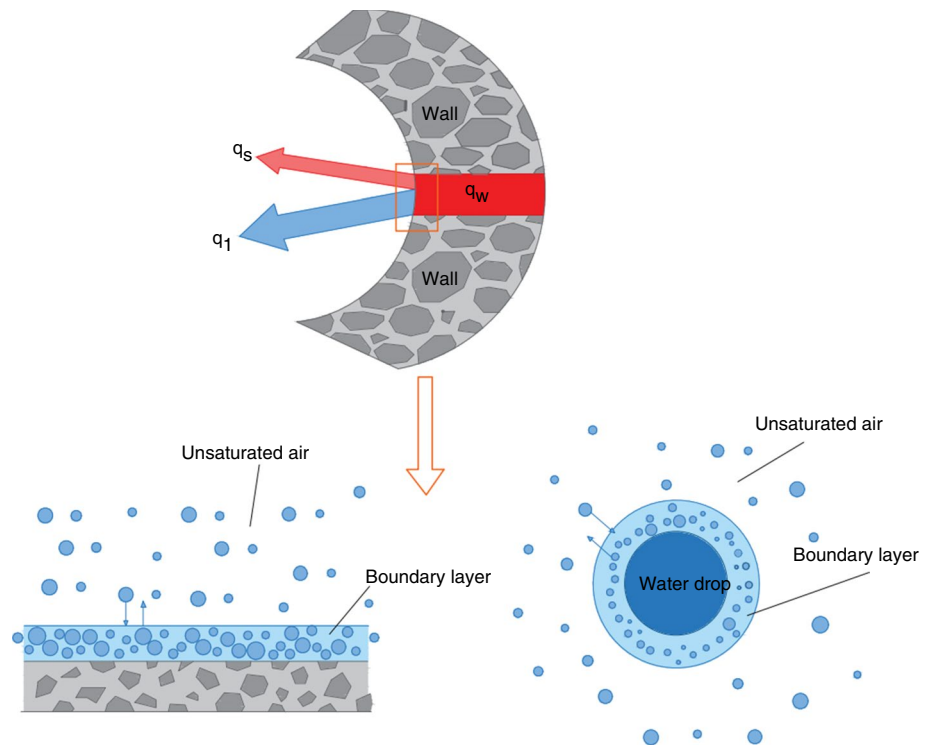


Table 5 Deep Mine Temperature and Humidity Chart [142–145]

Mine	Working face level/m	Air temperature/K	Relative humidity /%
Zhangxiaolou	−1000	307	95
Zhangshuanglou	−1200	307–309	95–100
Jiahe	−800	307	Almost 100
Zhouyuanshan	−650	303	95
Sanhejian	−980	308	94.2
Fenglong	−900	304	84
Jisan	−880	305.5	92

improving the damp-heat conditions and seeking cooling and dehumidification measures [40, 155].

In 1981, Hou [156] first proposed the view that the heat released by the surrounding rock and absorbed by the wind flow should include two parts: sensible heat exchange and latent heat exchange, and pointed out the fact that there is moisture exchange between the wind flow and the surrounding rock. The theory of heat and moisture exchange between wind flow and surrounding rock includes three processes: heat conduction inside the rock, convective heat transfer between rock and wind flow, and convective mass transfer between rock and wind flow. The heat released by the surrounding rock (Eq. 28) is partly used to consume the latent heat of water evaporation on the wall, and partly used to be the sensible heat used for wind flow, as shown in Fig. 26 [157].

$$q_w = q_s + q_l \quad (28)$$

where, q_w is the total heat flux density that dissipates heat from the surrounding rock to the wind flow, $\text{J}\cdot\text{m}^{-2}\cdot\text{s}^{-1}$; q_s is the sensible heat flow density entering the wind flow from the surrounding rock wall, $\text{J}\cdot\text{m}^{-2}\cdot\text{s}^{-1}$; q_l is the latent heat flow density entering the wind flow from the surrounding rock wall, $\text{J}\cdot\text{m}^{-2}\cdot\text{s}^{-1}$.

As for the influence of the damp-heat environment in the mine, scholars often analyze the damp-heat influence on the wind flow of the rock from the sensible heat and latent heat of the damp-hot surrounding rock, that is, only the water evaporation of the surrounding rock is considered. On this basis, Gao [158] considered the influence of water evaporation factors in the wind flow on the humid and hot environment of the mine, the sensible heat (Eq. 29) emitted by the surrounding rock wall into the wind is partly used to increase the temperature of the wind flow and partly used for the heat absorbed by the water evaporation in the wind flow.

$$q_s = q_f + q_t \quad (29)$$

where, q_s is the sensible heat flow density entering the wind flow from the surrounding rock wall, $\text{J}\cdot\text{m}^{-2}\cdot\text{s}^{-1}$; q_f is the sensible heat that increases the air flow temperature, $\text{J}\cdot\text{m}^{-2}\cdot\text{s}^{-1}$; q_t is the latent heat required for the evaporation of water in the wind, $\text{J}\cdot\text{m}^{-2}\cdot\text{s}^{-1}$.

The high temperature and high humidity environment of deep well mining have become an important factor restricting mine production, and the use of a fan is the most common way to improve the underground wet and hot environment conditions. Due to the increase in underground mining depth, the temperature of the air inlet of the fan is too high, and it is difficult to transport air at the appropriate temperature to the working face, which makes the cooling and dehumidification work efficiency low. Therefore, how to reduce the inlet air temperature has become a new research topic.

To this end, this paper proposes a new scheme design of the cooling fan system, the core of the scheme is the research and design of a fan cooling exchanger, the low-temperature water of the mine can be used to absorb the heat of the air flow, reduce the air flow temperature, and transport the geothermal air flow to the working surface, so as to reduce the temperature of the deep mining face and create a good working environment.

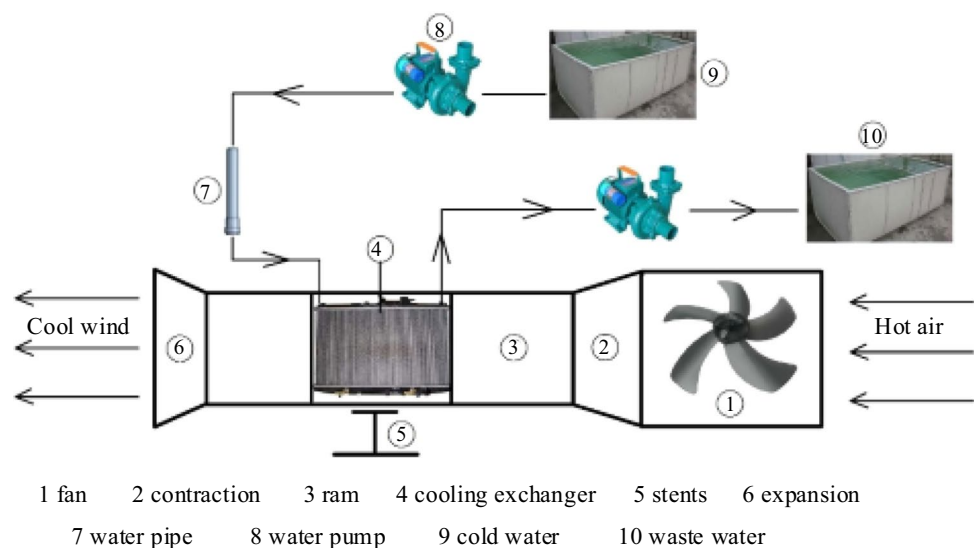
Design principle of cooling exchanger

As an important part of the cooling fan system, the cooling exchanger has the advantages of reducing air flow temperature, low cost, simple equipment, and effectively improving the operating environment of deep Wells. It is a technical measure put forward after years of experience accumulation and working practice, and it is very feasible. The schematic diagram of the scheme is shown in Fig. 27, the fan, cooling exchanger, and cooling water circulation circuit in the figure form a complete cooling fan system. According to the need to meet the deep well working requirements of the temperature range, the design of cooling system components, including heat exchanger heat transfer area, heat exchanger size, cooling capacity, pump flow and power, fan flow rate

and other parameters, among which, the design of cooling exchanger is one of the important links.

According to the layout requirements of the cooling system in the mine, the cooling exchanger should be arranged in front of the fan, and its layout space is limited. It is the basic requirement of cooling exchanger design to increase the heat transfer rate of the fin surface and control the volume of the cooling exchanger. The improvement of the heat transfer rate of the cooling exchanger mainly depends on two aspects. On the one hand, the fin surface heat transfer should be strengthened to improve the heat transfer coefficient, so as to improve the heat transfer performance of the cooling exchanger. On the other hand, the cooling exchanger structure and the corresponding fin structure parameters are optimized to improve the cooling performance of the cooling exchanger. The improvement of the heat transfer rate of the cooling exchanger mainly depends on two aspects. On the one hand, the fin surface heat transfer should be strengthened to improve the heat transfer coefficient, so as to improve the heat transfer performance of the cooling exchanger. On the other hand, the cooling exchanger structure and the corresponding fin structure parameters are optimized to improve the cooling performance of the cooling exchanger. With the development of high power, low fuel consumption and lightweight, the design of cooling exchangers is also moving toward compact and high efficiency. In addition to the application of new materials, the structure of the cooling exchanger also plays a crucial role in optimizing the cooling exchanger structure to improve its structural performance while reducing the mass of the parts. By changing the fin structure of the cooling exchanger, the heat exchange efficiency of the fin surface of the cooling exchanger is improved to achieve the increase in heat exchange per unit area, and the predetermined heat dissipation performance is achieved with a smaller volume of the cooling exchanger, so

Fig. 27 Schematic diagram of cooling system



as to save manufacturing materials and reduce manufacturing costs.

Research on cooling exchangers based on field cooperation theory

Feasibility analysis

Since the field synergy theory was put forward, its theory has gradually developed and matured, the depth of the research has changed from the initial research of laminar ideal fluid to the exploration that can be used to solve the actual turbulent fluid, and the breadth of research has gradually changed from the initial analysis of the essence of heat transfer enhancement to the study of mass transfer theory and the study of heat-mass transfer in more complex situations. The derivation of each theoretical equation, and the exploration of the synergistic effect of the velocity field, the temperature gradient field, and the concentration gradient field, all reflect a solid theoretical foundation for field synergy. Under the guidance of the mature field synergy theory, many scholars have begun to solve practical engineering problems. Among them, the use of the field synergy theory to improve the enhanced heat transfer performance of heat exchangers is the most extensive, from the design of channel and fin to the synergistic action with desiccant. In addition, the field synergy theory has also been widely researched and developed in other fields, including nanofluids, combustion reactors, screw plasticizing systems and COHP for heat transfer applications, POC devices and seawater desalination adsorption systems for mass transfer applications, and the CWCT devices and CVD devices for heat-mass synergy applications; All these researches have proved that the theory of field synergy can be used to solve practical problems in engineering applications and provide guidance for improving the efficiency of heat and mass transfer.

It has always been the goal of mine researchers to study the damp-heat mechanism of the mine and improve the underground working environment. It is a good way to improve the underground working environment by installing a cooling exchanger at the end of the fan working in a deep well, and the structure design of the cooling exchanger is an extremely important part of the design of the cooling system at the end of the fan. The design of a cooling heat exchanger is mainly to design the fin structure, which can improve the heat transfer efficiency of the fin surface of the cooling exchanger, and realize the increase of heat transfer per unit area.

The field synergy theory can be used to explore the essence of heat and mass transfer to enhance its transfer effect, the working principle of cooling heat exchanger is the heat and moisture exchange process between cooling water and underground high temperature and humidity, which has

extremely high similarity and adaptability with the research content of the field synergy theory. Therefore, it is of certain research significance to apply the theory of field synergy to the study of the structural design of cooling exchangers in deep wells, to explore the mechanism of underground wet and heat transfer, and to improve the underground moisture and heat environment.

Preliminary study on the structural design of cooling exchanger based on the theory of field synergy

(1) Analysis of heat transfer mechanism of different cooling exchanger fin structures.

In the existing research, the fin structure of heat exchangers is diverse, and it needs a long and complicated process and cycles to study and explore the fin in different categories. As the first exploration of analyzing deep well cooling exchanger based on field cooperation principle, starting with the study of the fin structure, this paper analyzes the synergistic effects of airflow velocity field and temperature gradient field, velocity field and moisture concentration gradient field, evaluate the influence of moisture and heat exchange with cooling water under the model conditions of the straight fin structure, H-shaped fin structure and H fin structure with open shutters (Fig. 28).

The distribution of airflow velocity field, temperature gradient field and water concentration gradient field under different fin structures are analyzed by numerical simulation, Because of the different structure features of the fins, when the wet hot air goes through the fin, the wind flow will be affected by different levels of resistance, which changes the direction of the wind, the corresponding, the angle between the velocity field and the temperature gradient and the angle between the velocity field and the concentration gradient has varying degrees of change. It is of great significance for the selection of the fin structure of the cooling exchanger to explore the degree of field synergy.

(2) Influence of fin structural parameters.

Through the above research on the heat transfer performance of cooling exchangers with different fin structures, the heat and humidity exchange between hot-wet air flow and cooling water under different air flow directions can be obtained, and from the perspective of field synergy theory, the situation that the minimum coordination angle means the best coordination effect is analyzed, so as to provide guidance for the design of fin structure of cooling exchangers. Taking the H-shaped louvered fin structure as an example, we can explore the influence of fin thickness and fin spacing on heat transfer performance. By analyzing the synergistic effect of each field under different fin thickness and fin spacing based on field synergistic theory, the setting of the exchanger can be optimized, the heat exchange efficiency of

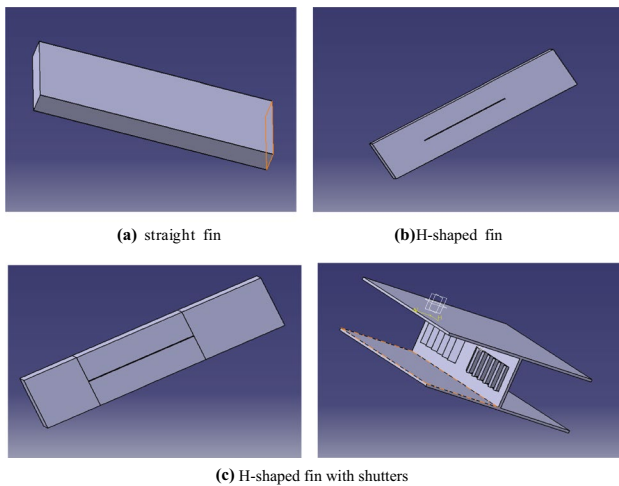


Fig. 28 Schematic diagram of cooling exchanger of the different fin structure

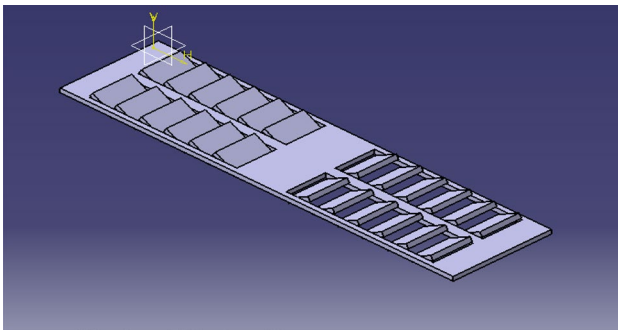


Fig. 29 The structure diagram of the louvered fin

hot-wet air and cooling water can be improved, and the inlet temperature of fan can be improved. Figure 29 shows the structure diagram of the louvered fin.

(3) Research on the optimization design of enhanced heat and mass transfer based on the combination of field synergy theory and ventilation system power consumption.

The research of cooling exchanger design based on field synergy theory can improve the heat and mass exchange between hot-wet air flow and cooling water and strengthen heat and mass transfer. However, in actual working conditions, factors such as cooling exchanger resistance, pressure drop, heat transfer coefficient of fin surface and exchanger cost need to be considered. At the same time, whether the optimal enhanced heat transfer condition is suitable for the environmental conditions of underground personnel is also one of the criteria to be measured. Therefore, it is our goal and focuses to combine the field synergy theory with the power consumption of ventilation system settings and explore the optimal design for improving and

strengthening heat and mass transfer to meet the demands of workers' working environment under the condition of reasonable power consumption.

The above-mentioned assumption of the idea of the cooling exchanger based on the field synergy theory is a preliminary exploration and attempt. It is only analyzed and optimized from the perspective of the structure of the fins. Many other factors affect the velocity field, temperature gradient field, and water concentration gradient field, such as air viscosity coefficient, frictional resistance, the number and arrangement of fins, etc., which can be used in subsequent research work.

Conclusions

- (1) Since the field synergy was proposed, its theory has gradually developed and matured. The properties of the fluid have been extended from laminar flow to more realistic turbulent flow, the applicable objects have also expanded from heat transfer enhancement to mass transfer and then to the synergy of heat-mass coupling, and the formulas were derived.
- (2) In the practical engineering application of the field synergy theory, enhancing the heat exchange performance of the heat exchanger is the most widely used; and it is also applied to various reactors, nanofluids, silica gel regeneration technology, seawater desalination technology, and other fields. It is a great guiding significance to optimize the design of the structures by improving the field synergy effect.
- (3) Reducing the inlet air flow temperature is an effective measure to improve the efficiency of underground heat transfer. It is a bold attempt to apply the field synergy theory to the research and development of the cooling exchanger under a high-temperature environment in a deep well. By analyzing its feasibility and exploring the fin structure and parameter design of the exchanger based on the field synergy theory, the exchanger structure with the best heat transfer performance can be selected.
- (4) In practical engineering applications, the optimal design of maximizing heat transfer and dehumidification with minimum power consumption can be obtained by combining field synergy theory with system power consumption.

Acknowledgements This work was supported by the National Science Foundation of China [51874187]; Shandong Natural Science Foundation [ZR2018MEE002]; Outstanding youth innovation team project in Shandong colleges and Universities [2019KJH008].

Author contributions All authors contributed to the study conception and design. MQ contributed to writing—original draft preparation. YZ contributed to conceptualization ideas. XZ contributed to methodology. HS contributed to investigation. CF contributed to writing—reviewing and editing. QY provided the software. SY contributed to visualization.

Code availability No data or code were used for the research described in the article. We have no include a data availability in our manuscript.

Declarations

Conflict of interest The authors declare that they have no known competing financial interests or personal relationships that could have appeared to influence the work reported in this paper.

Consent to publications I would like to declare on behalf of my co-authors that this article has not been published previously and is not being submitted for publication elsewhere. We hereby confirm that this manuscript is our original work. If this article was accepted, we confirm that it will not be published elsewhere in the same form, in English or any other language, without the written consent of the publisher.

References

- He YL, Tao WQ, Qu ZG, Chen ZQ. Steady natural convection in a vertical cylindrical envelope with adiabatic lateral wall. *Int J Heat Mass Transf.* 2004;47(14–16):3131–44. <https://doi.org/10.1016/j.ijheatmasstransfer.2004.02.016>.
- Mehrali M, Ghatkesar MK, Pecnik R. Full-spectrum volumetric solar thermal conversion via graphene/silver hybrid plasmonic nanofluids. *Appl Energy.* 2018;224:103–15. <https://doi.org/10.1016/j.apenergy.2018.04.065>.
- Murshed SMS, Nieto de Castro CA. Conduction and convection heat transfer characteristics of ethylene glycol based nanofluids – A review. *Appl Energy.* 2016;184:681–95. <https://doi.org/10.1016/j.apenergy.2016.11.017>.
- Zhang Y, Li HN, Li C, Huang C, Ali HM, Xu X, Mao C, Ding W, Cui X, Yang M, et al. Nano-enhanced biolubricant in sustainable manufacturing: From processability to mechanisms. *Friction.* 2022;10(6):803–41. <https://doi.org/10.1007/s40544-021-0536-y>.
- Wang X, Li C, Zhang Y, Ali HM, Sharma S, Li R, Yang M, Said Z, Liu X. Tribology of enhanced turning using biolubricants: a comparative assessment. *Tribol Int.* 2022. <https://doi.org/10.1016/j.triboint.2022.107766>.
- Yang M, Li C, Zhang Y, Wang Y, Li B, Jia D, Hou Y, Li R. Research on microscale skull grinding temperature field under different cooling conditions. *Appl Therm Eng.* 2017;126:525–37. <https://doi.org/10.1016/j.applthermaleng.2017.07.183>.
- Guo ZY, Li DY, Wang BX. A novel concept for convective heat transfer enhancement. *Int J Heat Mass Transf.* 1998;41(14):2221–5.
- Guo Z. Mechanism and control of convective heat transfer—Coordination of velocity and heat flow fields. *Chin Sci Bull.* 2001;7:4.
- Wang S, Z, Li X, Z., Guo Y. Novel concept and device of heat transfer augmentation. *Heat Transfer Conference.* 1998.
- He Y-L, Tao W-Q. Numerical studies on the inherent interrelationship between field synergy principle and entransy dissipation extreme principle for enhancing convective heat transfer. *Int J Heat Mass Transf.* 2014;74:196–205. <https://doi.org/10.1016/j.ijheatmasstransfer.2014.03.013>.
- Tao W, Guo Z, Wang B. Field synergy principle for enhancing convective heat transfer - Its extension and numerical verifications. *Int J Heat Mass Transf.* 2002;45(18):3849–56.
- Tao WQ, He YL, Wang QW. A unified analysis on enhancing single phase convective heat transfer with field synergy principle. *Int J Heat Mass Transf.* 2002;45(24):4871–9.
- He YL, Tao WQ, Song FQ, Zhang W. Three-dimensional numerical study of heat transfer characteristics of plain plate fin-and-tube heat exchangers from view point of field synergy principle. *Int J Heat Fluid Flow.* 2005;26(3):459–73. <https://doi.org/10.1016/j.ijheatfluidflow.2004.11.003>.
- Guo ZY, Tao WQ, Shah RK. The field synergy (coordination) principle and its applications in enhancing single phase convective heat transfer. *Int J Heat Mass Transf.* 2005;48(9):1797–807. <https://doi.org/10.1016/j.ijheatmasstransfer.2004.11.007>.
- Hua Y-C, Zhao T, Guo Z-Y. Optimization of the one-dimensional transient heat conduction problems using extended entransy analyses. *Int J Heat Mass Transf.* 2018;116:166–72. <https://doi.org/10.1016/j.ijheatmasstransfer.2017.08.101>.
- Wu L, Li Z, Song Y. Field synergy principle of heat and mass transfer. *Sci Bull.* 2009;54(24):4604–9. <https://doi.org/10.1007/s11434-009-0498-3>.
- Mehra B, Simo Tala JV, Habchi C, Harion JL. Local field synergy analysis of conjugate heat transfer for different plane fin configurations. *Appl Therm Eng.* 2018;130:1105–20. <https://doi.org/10.1016/j.applthermaleng.2017.11.064>.
- Zuo Q, Li Q, Yang X, Chen W, Zhu G, Shen Z, Xie Y, Tang Y. Investigation of electrically heating catalytic converter flow and temperature field performance improvement based on field synergy. *Energy.* 2023. <https://doi.org/10.1016/j.energy.2023.127360>.
- Kuo J-K, Yen T-S, Co-K C. Improvement of performance of gas flow channel in PEM fuel cells. *Energy Convers Manag.* 2008;49:2776–87. <https://doi.org/10.1016/j.enconman.2008.03.024>.
- Zhang Y, Zhang X, Li M, Liu Z. Research on heat transfer enhancement and flow characteristic of heat exchange surface in cosine style runner. *Heat Mass Transf.* 2019;55(11):3117–31. <https://doi.org/10.1007/s00231-019-02647-5>.
- Hao J, Chen J, Ma T, Hao T, Zhou J, Du X. Flow channel structure optimization and analysis of proton exchange membrane fuel cell based on the finite data mapping and multi-field synergy principle. *Int J Heat and Mass Transf.* 2023. <https://doi.org/10.1016/j.ijheatmasstransfer.2023.123997>.
- Wu X, Zhang W, Gou Q, Luo Z, Lu Y. Numerical simulation of heat transfer and fluid flow characteristics of composite fin. *Int J Heat Mass Transf.* 2014;75:414–24. <https://doi.org/10.1016/j.ijheatmasstransfer.2014.03.087>.
- Li J, Ling X, Peng H. Field synergy analysis on convective heat transfer and fluid flow of a novel triangular perforated fin. *Int J Heat Mass Transf.* 2013;64:526–35. <https://doi.org/10.1016/j.ijheatmasstransfer.2013.04.039>.
- Li J, Peng H, Ling X. Numerical study and experimental verification of transverse direction type serrated fins and field synergy principle analysis. *Appl Therm Eng.* 2013;54(1):328–35. <https://doi.org/10.1016/j.applthermaleng.2013.01.027>.
- Jin Y, Tang G-H, He Y-L, Tao W-Q. Parametric study and field synergy principle analysis of H-type finned tube bank with 10 rows. *Int J Heat Mass Transf.* 2013;60:241–51. <https://doi.org/10.1016/j.ijheatmasstransfer.2012.11.043>.
- Min CH, He YL, Liu XL, Yin BH, Jiang W, Tao WQ. Parameter sensitivity examination and discussion of PEM fuel cell simulation model validation. *J Power Sources.* 2006;160(1):374–85. <https://doi.org/10.1016/j.jpowsour.2006.01.080>.
- Sun XY, Hua LJ, Dai YJ, Ge TS, Wang RZ. Field synergy analysis on heat and moisture transfer processes of desiccant

- coated heat exchanger. *Int J Thermal Sci.* 2021. <https://doi.org/10.1016/j.ijthermalsci.2021.106889>.
28. Zhao TS, Song YJ. Forced convection in a porous medium heated by a permeable wall perpendicular to flow direction: analyses and measurements. *Int J Heat Mass Transf.* 2001;44(5):1031–7.
 29. Jia GH, Dai L, Li LJ, Tian GS, Gao ZC. Field synergy analysis of the combustion process of a biomass rotary burner. *J Central South Univ.* 2021;52:168–75.
 30. Zhang X, Zhang X, Bao C, Lai N-C. Numerical study and field synergy analysis on CO selective methanation packed-bed reactor. *Int J Hydrogen Energy.* 2022. <https://doi.org/10.1016/j.ijhydene.2022.11.042>.
 31. Liu Y, Dong Y, Xie L-t, Zhang C-z, Xu C. Heat transfer enhancement of supercritical CO₂ in solar tower receiver by the field synergy principle. *Appl Therm Eng.* 2022. <https://doi.org/10.1016/j.applthermaleng.2022.118479>.
 32. Long R, Li M, Chen X, Liu Z, Liu W. Synergy analysis for ion selectivity in nanofluidic salinity gradient energy harvesting. *Int J Heat and Mass Transf.* 2021. <https://doi.org/10.1016/j.ijheatmasstransfer.2021.121126>.
 33. Jian R, Yang W, Cheng L, Xie P. Numerical analysis of enhanced heat transfer by incorporating torsion elements in the homogenizing section of polymer plasticization with the field synergy principle. *Int J Heat Mass Transf.* 2017;115:946–53. <https://doi.org/10.1016/j.ijheatmasstransfer.2017.07.121>.
 34. Jiaqiang E, Zhao X, Liu H, Chen J, Zuo W, Peng Q. Field synergy analysis for enhancing heat transfer capability of a novel narrow-tube closed oscillating heat pipe. *Appl Energy.* 2016;175:218–28. <https://doi.org/10.1016/j.apenergy.2016.05.028>.
 35. Chen Q, Meng J-a. Field synergy analysis and optimization of the convective mass transfer in photocatalytic oxidation reactors. *Int J Heat and Mass Transf.* 2008;51:2863–70.
 36. Li M, Zhao Y, Long R, Liu Z, Liu W. Field synergy analysis for heat and mass transfer characteristics in adsorption-based desalination and cooling systems. *Desalination.* 2021. <https://doi.org/10.1016/j.desal.2021.115244>.
 37. Xie X, He C, Zhang B, Chen Q. Heat transfer enhancement for the coil zone of closed wet cooling towers through field synergy analysis. In: 13th International Symposium on Process Systems Engineering (PSE 2018). edn.1927–1932.
 38. An L, Zhang T, Lei X, Yang P, Liu Y. Local heat and mass transfer characteristics of different channel configurations in polysilicon chemical vapor deposition reactor. *Sol Energy.* 2020;196:494–504. <https://doi.org/10.1016/j.solener.2019.12.059>.
 39. Sasmito AP, Kurnia JC, Birgersson E, Mujumdar AS. Computational evaluation of thermal management strategies in an underground mine. *Appl Therm Eng.* 2015;90:1144–50. <https://doi.org/10.1016/j.applthermaleng.2015.01.062>.
 40. Ryan A, Euler DS. Heat stress management in underground mines. *Int J Min Sci Technol.* 2017;27(4):651–5. <https://doi.org/10.1016/j.ijmst.2017.05.020>.
 41. He MC, Guo PY, Chen XQ, Meng L, Zhu YY. Characteristics of high temperature body in deep well of Sanhejian Mine and its heat damage control method. *Chin J Rock Mech Eng.* 2010;29(S1):2593–7 ((in Chinese)).
 42. Zhang XJ, Ji JH, Chen W. Thermal analysis of surrounding rock in deep thermal mine. *Coal Mining Technol.* 2009;14:5–13.
 43. Qu M, Zhang Y, Zhang X, Jia Y, Fu C, Yao Q, Cao J. A review: Analysis and development of heat–mass synergy theory. *Energy Rep.* 2022;8:14830–51. <https://doi.org/10.1016/j.egyr.2022.11.021>.
 44. Meng J-A, Liang X-G, Li Z-X. Field synergy optimization and enhanced heat transfer by multi-longitudinal vortexes flow in tube. *Int J Heat Mass Transf.* 2005;48(16):3331–7. <https://doi.org/10.1016/j.ijheatmasstransfer.2005.02.035>.
 45. Liu W, Liu Z, Guo Z. Physical quantity synergy in laminar flow field of convective heat transfer and analysis of heat transfer enhancement. *Sci Bull.* 2009;54(19):3579–86. <https://doi.org/10.1007/s11434-009-0223-2>.
 46. Liu W, Liu ZC, Huang SY. Physical quantity synergy in the field of turbulent heat transfer and its analysis for heat transfer enhancement. *Chin Sci Bull.* 2010;23:2589–97.
 47. Liu W, Liu P, Dong ZM, Yang K, Liu ZC. A study on the multi-field synergy principle of convective heat and mass transfer enhancement. *Int J Heat Mass Transf.* 2019;134:722–34. <https://doi.org/10.1016/j.ijheatmasstransfer.2019.01.077>.
 48. Cao Y, Ke H, Lin Y, Zeng M, Wang Q. Investigation on the flow noise propagation mechanism in pipelines of shell-and-tube heat exchangers based on synergy principle of flow and sound fields. *Appl Therm Eng.* 2017;122:339–49. <https://doi.org/10.1016/j.applthermaleng.2017.04.057>.
 49. Tao W-Q, He Y-L, Chen L. A comprehensive review and comparison on headline concept and field synergy principle. *Int J Heat Mass Transf.* 2019;135:436–59. <https://doi.org/10.1016/j.ijheatmasstransfer.2019.01.143>.
 50. Vohra A, Goswami DY, Deshpande DA, Block SS. Enhanced photocatalytic disinfection of indoor air. *Applied Catalysis B: Environmental.* 2006;
 51. Zhang Y, Li M. Research on flow and heat transfer characteristics of heat transfer surface of trapezoidal duct. *Heat Mass Transf.* 2019;56(5):1475–86. <https://doi.org/10.1007/s00231-019-02794-9>.
 52. Zhang X, Zhang Y, Liu Z, Liu J. Analysis of heat transfer and flow characteristics in typical cambered ducts. *Int J Therm Sci.* 2020. <https://doi.org/10.1016/j.ijthermalsci.2019.106226>.
 53. Guo J, Xu M, Cheng L. Numerical investigations of circular tube fitted with helical screw-tape inserts from the viewpoint of field synergy principle. *Chem Eng Process.* 2010;49(4):410–7. <https://doi.org/10.1016/j.ccep.2010.02.011>.
 54. Yu Y, Wang H, Song M, Meng H, Wang Z, Wu J. The effects of element direction and intersection angle of adjacent Q-type inserts on the laminar flow and heat transfer. *Appl Therm Eng.* 2016;94:282–95. <https://doi.org/10.1016/j.applthermaleng.2015.10.092>.
 55. Guo J, Huai X. Numerical investigation of helically coiled tube from the viewpoint of field synergy principle. *Appl Therm Eng.* 2016;98:137–43. <https://doi.org/10.1016/j.applthermaleng.2015.12.012>.
 56. Wu JM, Tao WQ. Investigation on laminar convection heat transfer in fin-and-tube heat exchanger in aligned arrangement with longitudinal vortex generator from the viewpoint of field synergy principle. *Appl Therm Eng.* 2007;27(14–15):2609–17. <https://doi.org/10.1016/j.applthermaleng.2007.01.025>.
 57. Yang J, Ma L, Liu J, Liu W. Thermal–hydraulic performance of a novel shell-and-tube oil cooler with multi-fields synergy analysis. *Int J Heat Mass Transf.* 2014;77:928–39. <https://doi.org/10.1016/j.ijheatmasstransfer.2014.06.015>.
 58. Guo J, Xu M, Cheng L. The application of field synergy number in shell-and-tube heat exchanger optimization design. *Appl Energy.* 2009;86(10):2079–87. <https://doi.org/10.1016/j.apenergy.2009.01.013>.
 59. Hamid MOA, Zhang B, Yang L. Application of field synergy principle for optimization fluid flow and convective heat transfer in a tube bundle of a pre-heater. *Energy.* 2014;76:241–53. <https://doi.org/10.1016/j.energy.2014.06.055>.
 60. Ma L-D, Li Z-Y, Tao W-Q. Experimental verification of the field synergy principle. *Int Commun Heat Mass Transf.* 2007;34(3):269–76. <https://doi.org/10.1016/j.icheatmasstransfer.2006.11.008>.

61. Wu JM, Tao WQ. Numerical study on laminar convection heat transfer in a channel with longitudinal vortex generator. Part B: Parametric study of major influence factors. *Int J Heat Mass Transf.* 2008;51:3683–92.
62. Wu JM, Tao WQ. Numerical study on laminar convection heat transfer in a rectangular channel with longitudinal vortex generator. Part A: verification of field synergy principle. *Int J Heat Mass Transf.* 2008;51:1179–91.
63. Shaeri MR, Jen T-C. The effects of perforation sizes on laminar heat transfer characteristics of an array of perforated fins. *Energy Convers Manage.* 2012;64:328–34. <https://doi.org/10.1016/j.enconman.2012.05.002>.
64. Deng Y, Zheng EJ W, Zhang B, Zhao X, Zuo Q, Zhang Z, Han D. Influence of geometric characteristics of a diesel particulate filter on its behavior in equilibrium state. *Appl Therm Eng.* 2017;123:61–73. <https://doi.org/10.1016/j.applthermaleng.2017.05.071>.
65. Chang S. Field synergy principle to square and trapezoid types fuel cell bipolar plate of mold injection. In: *Power & Energy Engineering Conference*: 2010; 2010.
66. Kuo J-K, Co-K C. Evaluating the enhanced performance of a novel wave-like form gas flow channel in the PEMFC using the field synergy principle. *J Power Sources.* 2006;162(2):1122–9. <https://doi.org/10.1016/j.jpowsour.2006.07.053>.
67. Hamid MOA, Zhang B. Field synergy analysis for turbulent heat transfer on ribs roughened solar air heater. *Renew Energy.* 2015;83:1007–19. <https://doi.org/10.1016/j.renene.2015.05.031>.
68. Yang YT, Chen CK, Chang SC, Sun SY. LBM simulations of channel flow with a cylinder by the field synergy principle. *Prog Comput Fluid Dynam Int J.* 2009;9(3–5):254–61.
69. Chen C-K, Yen T-S, Yang Y-T. Lattice Boltzmann method simulation of a cylinder in the backward-facing step flow with the field synergy principle. *Int J Therm Sci.* 2006;45(10):982–9. <https://doi.org/10.1016/j.ijthermalsci.2005.12.009>.
70. Zhang EJ B, Gong J, Yuan W, Zuo W, Li Y, Fu J. Multidisciplinary design optimization of the diesel particulate filter in the composite regeneration process. *Appl Energy.* 2016;181:14–28. <https://doi.org/10.1016/j.apenergy.2016.08.051>.
71. Jiaqiang E, Zhao X, Xie L, Zhang B, Chen J, Zuo Q, Han D, Hu W, Zhang Z. Performance enhancement of microwave assisted regeneration in a wall-flow diesel particulate filter based on field synergy theory. *Energy.* 2019;169:719–29. <https://doi.org/10.1016/j.energy.2018.12.086>.
72. Zhang L, Li J, Li Y, Wu J. Field synergy analysis for helical ducts with rectangular cross section. *Int J Heat Mass Transf.* 2014;75:245–61. <https://doi.org/10.1016/j.ijheatmasstransfer.2014.03.062>.
73. Zhang B, Hamid MOA, Liu W. Numerical and experimental study of field synergy analysis in water jet impingement based on minimum entropy generation method. *Appl Therm Eng.* 2016;99:944–58. <https://doi.org/10.1016/j.applthermaleng.2016.01.157>.
74. Habchi C, Lemenand T, Della Valle D, Pacheco L, Le Corre O, Peerhossaini H. Entropy production and field synergy principle in turbulent vortical flows. *Int J Therm Sci.* 2011;50(12):2365–76. <https://doi.org/10.1016/j.ijthermalsci.2011.07.012>.
75. Chen CO. Lattice Boltzmann method simulation of channel flow with square pillars inside by the field synergy principle. *Comput Model Eng Sci.* 2007;22(3):203–15.
76. Zhang B, Gong J-k, J-q E, Li Y. Failure recognition of the diesel particulate filter based on catastrophe theory. *Can J Chem Eng.* 2016;94(3):596–602. <https://doi.org/10.1002/cjce.22424>.
77. Chen Q, Ren J, Meng J-a. Field synergy equation for turbulent heat transfer and its application. *Int J Heat and Mass Transf.* 2007;50(25–26):5334–9. <https://doi.org/10.1016/j.ijheatmasstransfer.2007.10.001>.
78. Li Y, Wang Z, Yang J, Liu H. Thermal and hydraulic characteristics of microchannel heat sinks with cavities and fins based on field synergy and thermodynamic analysis. *Appl Therm Eng.* 2020. <https://doi.org/10.1016/j.applthermaleng.2020.115348>.
79. Guo Z-Y, Li Z-X. Size effect on single-phase channel flow and heat transfer at microscale. *Int J Heat Fluid Flow.* 2003;24(3):284–98. [https://doi.org/10.1016/s0142-727x\(03\)00019-5](https://doi.org/10.1016/s0142-727x(03)00019-5).
80. Dehghan M, Daneshpour M, Valipour MS, Rafee R, Saedodin S. Enhancing heat transfer in microchannel heat sinks using converging flow passages. *Energy Convers Manage.* 2015;92:244–50. <https://doi.org/10.1016/j.enconman.2014.12.063>.
81. Tang GH, Li XF, He YL, Tao WQ. Electroosmotic flow of non-Newtonian fluid in microchannels. *J Nonnewton Fluid Mech.* 2009;157(1–2):133–7. <https://doi.org/10.1016/j.jnnfm.2008.11.002>.
82. Zhao EJ X, ZhangChenLiaoZhangLengHanHu ZJGFEDW. A review on heat enhancement in thermal energy conversion and management using field synergy principle. *Appl Energy.* 2020. <https://doi.org/10.1016/j.apenergy.2019.113995>.
83. Sun XY, Dai YJ, Ge TS, Zhao Y, Wang RZ. Comparison of performance characteristics of desiccant coated air-water heat exchanger with conventional air-water heat exchanger – Experimental and analytical investigation. *Energy.* 2017;137:399–411.
84. Liang CP, Ture F, Dai YJ, Wang RZ, Ge TS. Experimental investigation on performance of desiccant coated microchannel heat exchangers under condensation conditions. *Energy Build.* 2021. <https://doi.org/10.1016/j.enbuild.2020.110622>.
85. Vivekh P, Kumja M, Bui DT, Chua KJ. Recent developments in solid desiccant coated heat exchangers – A review. *Appl Energy.* 2018;229:778–803. <https://doi.org/10.1016/j.apenergy.2018.08.041>.
86. Vivekh P, Bui DT, Kumja M, Islam MR, Chua KJ. Theoretical performance analysis of silica gel and composite polymer desiccant coated heat exchangers based on a CFD approach. *Energy Convers Manage.* 2019;187:423–46. <https://doi.org/10.1016/j.enconman.2019.02.093>.
87. Dai YJ, Wang RZ, Zhang HF. Parameter analysis to improve rotary desiccant dehumidification using a mathematical model. *Int J Therm Ences.* 2001;40(4):400–8.
88. Sphaier LA, Nóbrega CEL. Parametric analysis of components effectiveness on desiccant cooling system performance. *Energy.* 2012;38(1):157–66. <https://doi.org/10.1016/j.energy.2011.12.019>.
89. Higashi T, Zhang L, Saikawa M, Yamaguchi M, Dang C, Hihara E. Theoretical and experimental studies on isothermal adsorption and desorption characteristics of a desiccant-coated heat exchanger. *Int J Refrig.* 2017;84:228–37. <https://doi.org/10.1016/j.ijrefrig.2017.09.007>.
90. Karmakar A, Prabakaran V, Zhao D, Chua KJ. A review of metal-organic frameworks (MOFs) as energy-efficient desiccants for adsorption driven heat-transformation applications. *Appl Energy.* 2020. <https://doi.org/10.1016/j.apenergy.2020.115070>.
91. Valarezo AS, Sun XY, Ge TS, Dai YJ, Wang RZ. Experimental investigation on performance of a novel composite desiccant coated heat exchanger in summer and winter seasons. *Energy.* 2019;166:506–18. <https://doi.org/10.1016/j.energy.2018.10.092>.
92. Zheng X, Wang R, Ma W. Dehumidification assessment for desiccant coated heat exchanger systems in different buildings and climates: fast choice of desiccants. *Energy Build.* 2020. <https://doi.org/10.1016/j.enbuild.2020.110083>.
93. Vivekh P, Bui DT, Wong Y, Kumja M, Chua KJ. Performance evaluation of PVA-LiCl coated heat exchangers for next-generation of energy-efficient dehumidification. *Appl Energy.*

- 2019;237:733–50. <https://doi.org/10.1016/j.apenergy.2019.01.018>.
94. Sun XY, Dai YJ, Ge TS, Zhao Y, Wang RZ. Heat and mass transfer comparisons of desiccant coated microchannel and fin-and-tube heat exchangers. *Appl Therm Eng.* 2019;150:1159–67. <https://doi.org/10.1016/j.applthermaleng.2019.01.071>.
 95. Liu L, Zeng T, Huang H, Kubota M, Kobayashi N, He Z, Li J, Deng L, Li X, Feng Y, et al. Numerical modelling and parametric study of an air-cooled desiccant coated cross-flow heat exchanger. *Appl Therm Eng.* 2020. <https://doi.org/10.1016/j.applthermaleng.2020.114901>.
 96. Zhu XW, Zhao JQ. Improvement in field synergy principle: More rigorous application, better results. *Int J Heat Mass Transf.* 2016;100:347–54. <https://doi.org/10.1016/j.ijheatmasstransfer.2016.05.003>.
 97. Xie XC, Zhang Y, He C, Xu T, Zhang BJ, Chen QL. Bench-scale experimental study on the heat transfer intensification of a closed wet cooling tower using aluminum oxide nanofluids. *Ind Eng Chem Res.* 2017;56(20):6022–34. <https://doi.org/10.1021/acs.iecr.7b00724>.
 98. Wang ZK, Zeng ZX, Xu YH. Synergistic numerical study of velocity field and temperature field in advanced swirl combustor. *J Propulsion Technol.* 2015;36(06):876–83 ((in Chinese)).
 99. Zeng ZX, Wang ZK, Tian JY, Xu YH. Multi-field collaborative analysis of advanced swirl combustor. *J Propulsion Technol.* 2015;36(12):1859–67.
 100. Jq E, Zhang SL, Bo XZ, Li YQ, Dong JD, Zhang B. Performance and field synergy analysis of alcohol-based fuel burners. *J South China Univ Technol.* 2011;39(08):66–71 ((in Chinese)).
 101. Kelly AL, Brown EC, Coates PD. The effect of screw geometry on melt temperature profile in single screw extrusion. *Polym Eng Sci.* 2006;46(12):1706–14. <https://doi.org/10.1002/pen.20657>.
 102. Rittidech S, Wannapakne S. Experimental study of the performance of a solar collector by closed-end oscillating heat pipe (CEOHP). *Appl Therm Eng.* 2007;27(11–12):1978–85. <https://doi.org/10.1016/j.applthermaleng.2006.12.005>.
 103. Rittidech S, Dangeton W, Soponronnarit S. Closed-ended oscillating heat-pipe (CEOHP) air-preheater for energy thrift in a dryer. *Appl Energy.* 2005;81(2):198–208.
 104. Meena P, Rittidech S, Poomsa-ad N. Closed-loop oscillating heat-pipe with check valves (CLOHP/CVs) air-preheater for reducing relative humidity in drying systems. *Appl Energy.* 2007;84(4):363–73. <https://doi.org/10.1016/j.apenergy.2006.09.009>.
 105. Wannapakne S, Chaiwong T, Dandee M, Prompakdee S. Hot air dryer with closed – loop oscillating heat pipe with check valves for reducing energy in drying process. *Procedia Eng.* 2012;32:77–82. <https://doi.org/10.1016/j.proeng.2012.01.1239>.
 106. Weng Y-C, Cho H-P, Chang C-C, Chen S-L. Heat pipe with PCM for electronic cooling. *Appl Energy.* 2011;88(5):1825–33. <https://doi.org/10.1016/j.apenergy.2010.12.004>.
 107. Devendiran DK, Amirtham VA. A review on preparation, characterization, properties and applications of nanofluids. *Renew Sustain Energy Rev.* 2016;60:21–40. <https://doi.org/10.1016/j.rser.2016.01.055>.
 108. Vinardell MP, Sordé A, Díaz J, Baccarin T, Mitjans M. Comparative effects of macro-sized aluminum oxide and aluminum oxide nanoparticles on erythrocyte hemolysis: influence of cell source, temperature, and size. *J Nanoparticle Res.* 2015. <https://doi.org/10.1007/s11051-015-2893-9>.
 109. Eastman JA, Choi SUS, Li S, Yu W, Thompson LJ. Anomalously increased effective thermal conductivities of ethylene glycol-based nanofluids containing copper nanoparticles. *Appl Phys Lett.* 2001;78(6):718–20. <https://doi.org/10.1063/1.1341218>.
 110. Das SK, Putra N, Thiesen P, Roetzel W. Temperature dependence of thermal conductivity enhancement for nanofluids. *J Heat Transf.* 2003;125(4):567.
 111. Kim SJ, Bang IC, Buongiorno J, Hu LW. Surface wettability change during pool boiling of nanofluids and its effect on critical heat flux. *Int J Heat Mass Transf.* 2007;50(19–20):4105–16. <https://doi.org/10.1016/j.ijheatmasstransfer.2007.02.002>.
 112. Zhang X, Liu B, Liu J, Wang X, Zhang H. Experimental and numerical analysis of heat transfer and flow characteristics in parabolic ducts. *Int J Heat and Mass Transf.* 2020. <https://doi.org/10.1016/j.ijheatmasstransfer.2019.118912>.
 113. Wang G, Qi C, Tang J. Natural convection heat transfer characteristics of TiO₂–H₂O nanofluids in a cavity filled with metal foam. *J Therm Anal Calorim.* 2020;141(1):15–24. <https://doi.org/10.1007/s10973-020-09471-8>.
 114. Noorbakhsh M, Ajarostaghi SSM, Zabolli M, Kiani B. Thermal analysis of nanofluids flow in a double pipe heat exchanger with twisted tapes insert in both sides. *J Therm Anal Calorim.* 2021;147(5):3965–76. <https://doi.org/10.1007/s10973-021-10738-x>.
 115. Wang P, Lv J, Bai M, Li G, Zeng K. The reciprocating motion characteristics of nanofluid inside the piston cooling gallery. *Powder Technol.* 2015;274:402–17. <https://doi.org/10.1016/j.powtec.2015.01.004>.
 116. Liu H, Bai M, Lv J, Wang P, Wang Y, Hu C. Heat transfer analysis of piston cooling using nanofluids in the gallery. *Micro & Nano Lett.* 2015;10(1):28–33. <https://doi.org/10.1049/mnl.2014.0432>.
 117. Peng W, Minli B, Jizu L, Chengzhi H, Yuyan W. Numerical study on the microflow mechanism of heat transfer enhancement in nanofluids. *Nanoscale Microscale Thermophys Eng.* 2014;18(2):113–36. <https://doi.org/10.1080/15567265.2013.856498>.
 118. Peng W, Jizu L, Minli B, Yuyan W, Chengzhi H. A Numerical Investigation of Impinging Jet Cooling with Nanofluids. *Nanoscale Microscale Thermophys Eng.* 2014;18(4):329–53. <https://doi.org/10.1080/15567265.2014.921749>.
 119. Yin X, Bai M, Hu C, Lv J. Molecular dynamics simulation on the effect of nanoparticle deposition and nondeposition on the nanofluid explosive boiling heat transfer. *Num Heat Transf, Part A: Appl.* 2018;73(8):553–64. <https://doi.org/10.1080/10407782.2018.1459135>.
 120. Yin X, Hu C, Bai M, Lv J. Molecular dynamics simulation on the effect of nanoparticles on the heat transfer characteristics of pool boiling. *Num Heat Transf, Part B: Fundament.* 2018;73(2):94–105. <https://doi.org/10.1080/10407790.2017.1420323>.
 121. Zhang X, Zhang Y. Heat transfer and flow characteristics of Fe₃O₄-water nanofluids under magnetic excitation. *Int J Therm Sci.* 2021. <https://doi.org/10.1016/j.ijthermalsci.2020.106826>.
 122. Zhang X, Zhang Y. Experimental study on enhanced heat transfer and flow performance of magnetic nanofluids under alternating magnetic field. *Int J Thermal Sci.* 2021. <https://doi.org/10.1016/j.ijthermalsci.2021.106897>.
 123. Yang J-C, Li F-C, Cai W-H, Zhang H-N, Yu B. On the mechanism of convective heat transfer enhancement in a turbulent flow of nanofluid investigated by DNS and analyses of POD and FSP. *Int J Heat Mass Transf.* 2014;78:277–88. <https://doi.org/10.1016/j.ijheatmasstransfer.2014.06.077>.
 124. Cui W, Mao D, Lin B, Yang J. Field synergy analysis on the mechanism of heat transfer enhancement by using nanofluids. *Case Stud Therm Eng.* 2019. <https://doi.org/10.1016/j.csite.2019.100554>.
 125. Obee TN, Brown RT. TiO₂ Photocatalysis for indoor air applications: effects of humidity and trace contaminant levels on the

- oxidation rates of formaldehyde, toluene, and 1,3-butadiene. *Environ Sci Technol.* 1995;29(5):1223–31.
126. Jo WK, Park JH, Chun HD. Photocatalytic destruction of VOCs for in-vehicle air cleaning. *J Photochem Photobiol A.* 2002;148(1):109–19.
 127. Yang R, Zhang Y, Xu Q, Mo J. A mass transfer based method for measuring the reaction coefficients of a photocatalyst. *Atmos Environ.* 2007;41(6):1221–9. <https://doi.org/10.1016/j.atmosenv.2006.09.043>.
 128. Zhang YP, Yang R, Xu QJ, Mo JH. Characteristics of photocatalytic oxidation of toluene, benzene, and their mixture. *J Air Waste Manag Assoc.* 2007;57(1):94–101. <https://doi.org/10.1080/10473289.2007.10465302>.
 129. Chen Q, Ren J, Guo Z. Fluid flow field synergy principle and its application to drag reduction. *Sci Bull.* 2008;53(11):1768–72. <https://doi.org/10.1007/s11434-008-0237-1>.
 130. An LS, Yang Z, Zhong GY, Liu YW. Improvement of heat and mass transfer performance in a polysilicon chemical vapor deposition reactor with field synergy principle. *Energy Procedia.* 2017;105:688–93. <https://doi.org/10.1016/j.egypro.2017.03.376>.
 131. Hua LJ, Ge TS, Wang RZ. A mathematical model to predict the performance of desiccant coated evaporators and condensers. *Int J Refrig.* 2020;109:188–207. <https://doi.org/10.1016/j.ijrefrig.2019.10.001>.
 132. Cheng X, Liang X. Discussion on the applicability of entropy generation minimization and entransy theory to the evaluation of thermodynamic performance for heat pump systems. *Energy Convers Manage.* 2014;80:238–42. <https://doi.org/10.1016/j.enconman.2014.01.008>.
 133. Zhao D. Transient growth of flow disturbances in triggering a Rijke tube combustion instability. *Combust Flame.* 2012;159(6):2126–37. <https://doi.org/10.1016/j.combustflame.2012.02.002>.
 134. Xu XM, Li RZ, Fu JQ, Jiang HB. Research on the heat flow field synergy of electric vehicle power cabin at different charge and discharge rates. *Appl Therm Eng.* 2017;117:397–408. <https://doi.org/10.1016/j.applthermaleng.2017.01.063>.
 135. Tang J, Meng F, Zhang Y. Common probability-based interactive algorithms for group decision making with normalized probability linguistic preference relations. *Fuzzy Optim Decis Making.* 2021;21(1):99–136. <https://doi.org/10.1007/s10700-021-09360-1>.
 136. Bei C, Zhang H, Yang F, Song S, Wang E, Liu H, Chang Y, Wang H, Yang K. Performance analysis of an evaporator for a diesel engine-organic rankine cycle (ORC) combined system and influence of pressure drop on the diesel engine operating characteristics. *Energies.* 2015;8(6):5488–515. <https://doi.org/10.3390/en8065488>.
 137. Zuo E, Liu P, Peng W, HQ. Field synergy analysis of the micro-cylindrical combustor with a step. *Appl Thermal Eng.* 2016;93:83–9. <https://doi.org/10.1016/j.applthermaleng.2015.09.028>.
 138. Li Y, Liu G, Rao Z, Liao S. Field synergy principle analysis for reducing natural convection heat loss of a solar cavity receiver. *Renew Energy.* 2015;75:257–65. <https://doi.org/10.1016/j.renene.2014.09.055>.
 139. Tao WQ, Cheng YP, Lee TS. The influence of strip location on the pressure drop and heat transfer performance of a slotted fin. *Numerical Heat Transfer Applications. Part A: Applications*(5):463–480.
 140. Xie XP. New method in deep well cooling technology. *Nonferrous Metals Sci Eng.* 1996;01:7–10 ((in Chinese)).
 141. Jing Z, Zhu N, Lu S. Productivity model in hot and humid environment based on heat tolerance time analysis. *Build Environ.* 2009;44(11):2202–7.
 142. Han Q, Zhang Y, Li K, Zou S. Computational evaluation of cooling system under deep hot and humid coal mine in China: a thermal comfort study. *Tunnel Underground Space Technol.* 2019;90:394–403.
 143. Guo P, He M, Zheng L, Zhang N. A geothermal recycling system for cooling and heating in deep mines. *Appl Therm Eng.* 2017;116:833–9.
 144. Yang X, Han Q, Pang J, Shi X, Hou D, Chao L. Progress of heat-hazard treatment in deep mines. *Min Sci Technol.* 2011;21(2):295–9.
 145. Sasmito, Agus P. Computational evaluation of thermal management strategies in an underground mine. *Applied Thermal Engineering.* 2015.
 146. Wang YJ, Zhou GQ, Wei YZ, Kuang LF, Wu L. Experimental study on evolution law of unsteady temperature field in deep roadway. *J China Univ Min Technol.* 2011;40(03):345–50 ((in Chinese)).
 147. Wang HW, Rong H. Study on equivalent thermal conductivity of composite rock masses under the effect of flow-heat coupling. *J China Coal Soc.* 2013;38:1781–5.
 148. Ji JH, Liao Q, Hu QT, Chu ZX, Zhang XJ. Heat transfer characteristics of impact jet in excavation face. *J China Coal Soc.* 2013;38:554–60.
 149. Prashant K, Jain S, Singh R-u. Analytical solution to transient asymmetric heat conduction in a multilayer annulus. *J Heat Transf.* 2008;131:11304–11304.
 150. Singh S, Jain PK, Rizwan-uddin. Analytical solution to transient heat conduction in polar coordinates with multiple layers in radial direction. *Int J Thermal Sci.* 2008;47(3):261–73.
 151. Dehghan M, Daneshpour M, Valipour MS, Rafee R, Saedodin S. Enhancing heat transfer in microchannel heat sinks using converging flow passages. *Energy Convers Manage.* 2015;92:244–50.
 152. Anderson R, Souza ED. Heat stress management in underground mines. *Int J Min Sci Technol.* 2017;27(4):5.
 153. Zhang XM, Li LF, Wang ZG. Analysis of heat damage in coal mine and prediction of air flow temperature. *J Liaoning Tech Univ (Natural Sci).* 2012;31(06):826–9 ((in Chinese)).
 154. Huang YP, Zhao YH. Evaluation method of mine ventilation system. *Safety in Coal Mines.* 1983;09:24–31 ((in Chinese)).
 155. Ou XY, Yang SQ, Yu BH, Wang YJ, Wang F, Wang L, et al. Mine thermal environment assessment and its application. *J China Univ Min Technol.* 2005;03:323–6.
 156. Hou QZ. Discussion on air temperature calculation in high temperature mine. *Coal Eng.* 1981;01:10–4 ((in Chinese)).
 157. Zhang XB. Calculation of heat dissipation and air flow temperature and humidity of surrounding rock in wet roadway. M D thesis, Henan Polytechnic University, Jiaozuo, Henan; 2007. (in Chinese).
 158. Gao JL, Xu W, Zhang XB. Water evaporation treatment in wells and influence of temperature and humidity on air flow. In: 2010(Shenyang) International Symposium on Security Science and Technology; 2010; Chian Liaoning Shenyang; 2010: 512–516. (in Chinese).

Publisher's Note Springer Nature remains neutral with regard to jurisdictional claims in published maps and institutional affiliations.

Springer Nature or its licensor (e.g. a society or other partner) holds exclusive rights to this article under a publishing agreement with the author(s) or other rightsholder(s); author self-archiving of the accepted manuscript version of this article is solely governed by the terms of such publishing agreement and applicable law.